第九版

内科学

総編集

杉本恒明
矢崎義雄

編集

小俣政男
水野美邦

伊藤貞嘉
岩本愛吉
岡　芳知
金倉　譲
島本和明
菅野健太郎
曽根三郎
永井良三
中尾一和
山本一彦

朝倉書店

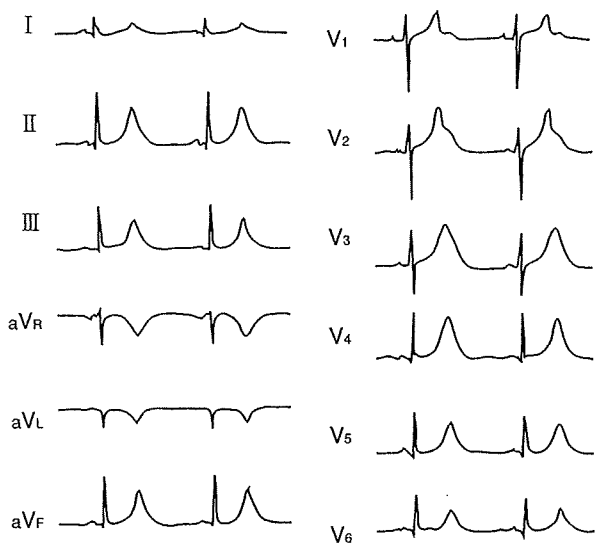

〈図 5-125〉先天性 QT 延長症候群の心電図
42 歳女性．長期にβ遮断薬投与が行われている．0.7 秒と著明な QT 延長を認める．

〈表 5-41〉先天性 QT 延長症候群の診断基準

		ポイント
心電図所見	A. QTc≧480 msec 1/2	3
	460～470 msec 1/2	2
	450 msec 1/2（男性）	1
	B. torsade de pointes	2
	C. 交代性 T 波（T wave alternan）	1
	D. notched T（3 誘導以上）	1
	E. 徐脈	0.5
臨床症状	A. 失神発作	
	ストレスに伴うもの	2
	ストレスに伴わないもの	1
	B. 先天性聾	0.5
家族歴	A. 確定診断を得た先天性 QT 延長症候群の家族歴があるもの	1
	B. 30 歳未満の突然死の家族歴があるもの	0.5

ポイントの合計により診断する．4 ポイント：診断確実，2 あるいは 3 ポイント：疑いあり，0 あるいは 1 ポイント：否定的（Schwartz, et al, 1993）．

【検査成績・診断・鑑別診断】

表 5-41 のような診断基準が設けられている．標準 12 誘導心電図，Holter 心電図，運動負荷心電図などの検査を行う．電気生理学的検査におけるプログラム刺激での torsade de pointes 誘発率は低く，診断的価値は少ない．β遮断薬などの治療効果を知ることも困難と考えられている．失神を生じる病態はいずれも鑑別の対象となる．

【経過・予後】

β遮断薬による治療が確立されていない時期の調査では，失神などの既往のある先天性 QT 延長症候群の年死亡率は 5% にものぼっていた．しかし，β遮断薬が投与されているものでは 10 年を経ても死亡率は 10% 以下にとどまる．また，男性の失神発作は少年期までに集中するが，女性では 30 歳をこえても失神が続く傾向があり，臨床像に性差がみられる．

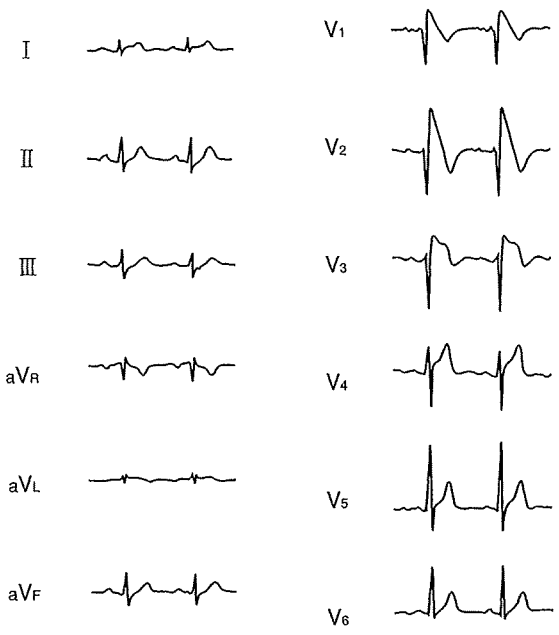

〈図 5-126〉Brugada 症候群が疑われる心電図
52 歳男性．V_1 と V_2 は coved 型に特有な ST-T 変化をみせている．診断は心電図所見のみでなく，家族歴や失神の既往を考慮する．

【治　療】

障害のあるイオンチャネルによって対処法は異なる．LQT 1 と LQT 2 では交感神経活動が torsade de pointes の出現を促進するため，β遮断薬が治療の主体となる．torsade de pointes の予防には高用量のβ遮断薬が必要となる．植え込み型除細動器や左星状神経節切除を要する症例もある．

(2) Brugada 症候群

【定義・概念】

1992 年，Brugada らは右胸部誘導の ST 上昇と右脚ブロックパターンを特徴とし，失神や突然死に至る疾患群を報告した．その家族性発症の傾向から遺伝性のある突然死関連疾患として注目されるようになった．

【原因・病因】

特徴的な心電図異常は右室流出路の活動電位の変化によって説明される．心筋の Na^+ チャネル遺伝子 SCN 5 A の変異が同定されたため，本疾患も遺伝子病としてとらえられている．なぜ活動電位の変化が右室に局在するのかなど未知のところが多い．

【疫学・臨床症状】

まれな疾患である．80% 以上が 30 歳～50 歳の男性であり，わが国を含む東南アジアに多い．失神，あるいは突然死として発症する．特記すべき身体所見を欠く．

【検査成績・診断・鑑別診断】

特徴的な心電図所見と心室細動，あるいはそれを示

唆する失神発作によって診断される．本人に心室細動を思わせるエピソードがないときは，血縁者の既往によって診断をする．V_1，V_2ではQRS終末部からST部分にかけて上に凸のときcoved型とよび（図5-126），ST上昇が下に凸ならsaddle-back型とよばれる．本症候群ではNa^+チャネル遮断薬や自律神経作動薬や遮断薬に対して特徴的な反応を示す．

不整脈源性右室心筋症（arrhythmogenic right ventricular cardiomyopathy; ARVC）を除外するためのMRI検査や，冠動脈攣縮（れんしゅく）の誘発を含む冠動脈造影も行われる．電気生理学的検査における心室細動の誘発頻度は報告により異なる．発作頻度によって重症度が決められるようにみえるが，初回発作でも致死的となるので重症度は測りにくい．

【経過・予後】

心室細動の既往がなくても心事故は4～8%に発生するという国外の報告はあるが，わが国ではこれよりも低い数値が報告されている．失神や突然死蘇生例では再発率が高い．

【治　療】

発作は心室細動として発症するために，通常の救急蘇生に準じる．速やかに電気的除細動を行わなければ致死的となる．本症候群の心電図異常は一部のNa^+チャネル遮断薬，β遮断薬，副交感神経刺激薬によって増悪する．これに対しβ刺激薬は心電図異常を改善させる．coved型のときに心室細動が生じやすい．薬物治療は不十分な効果しか望めず，しばしば植え込み型除細動器が選択される．〔村川裕二〕

■文　献

Sarkozy A, Brugada P: Sudden cardiac death and inherited arrhythmia syndromes. *J Cardiovasc Electrophysiol*, 16 (Suppl 1): S 8-20, 2005.

Schwartz PJ: The congenital long QT syndromes from genotype to phenotype: clinical implications. *J Intern Med*, 259: 39-47, 2006.

Schwartz PJ, Moss AJ, et al: Diagnostic criteria for the long QT syndrome. An update. *Circulation*, 88: 782-784. 1993.

5-6 虚血性心疾患 ischemic heart disease

1）冠血流調節と心筋虚血

(1) 冠循環調節機構

a. 冠循環の解剖

心筋に血液を供給する冠循環は，大動脈起始部から直径2～5 mmの左右3冠動脈が心外膜側を走行する．その3冠動脈から直径1 mm以下の小動脈となって心筋層内に入り，さらに冠動脈造影上判読不能となる直径数百μm以下の細動脈，中膜平滑筋が不連続となるメタ細動脈，毛細血管前細動脈を経て，内皮細胞と基底膜とからなる直径8～10μmの毛細血管へと移行する．そして毛細血管後細静脈を経て，直径数百μm前後の細静脈から，大部分は冠静脈洞を経て右房に還流する．一般に，細動脈から細静脈までの心筋層内の冠循環は冠微小循環とよばれ，抵抗血管として生理的な状態での冠循環調節の主役をなしている．

b. 冠循環の特徴と調節機構

冠循環の第1の特徴として，心臓はエネルギー消費の最も大きな臓器であるため，大量の血液供給を必要とする（安静時約1 ml/g/分）．しかし，他臓器への分配血液量の低下を避けることから必要最小限に抑えられている（心拍出量の約5%）．そのため，冠動脈狭窄などにより冠血流供給が制限されると，心筋は容易に虚血に陥る．

第2の特徴として，収縮期に高圧となる心内膜側は，心外膜側と比較して十分な組織灌流が得られにくいとされる．冠動脈狭窄などで冠血流が低下すると，心内膜側・心外膜側血流比は容易に0.7くらいまで低下し，心内膜側より容易に虚血が生ずる（wavefront現象）．

第3の特徴として，冠循環は脳循環とともに多少の灌流圧の変動にかかわらず冠血流量を維持する自己調節能（autoregulation）を有する点で，他臓器とは異なっている．冠微小血管トーヌスは，おもに平滑筋自体の特性にて制御されているが，神経・体液性因子の影響も受ける．

c. 冠微小血管トーヌスの神経性調節

冠動脈は全身の動脈のなかで最も豊富に神経が分布し，precapillaryレベルまで神経支配を受けており，冠血流量の調節を担っている．冠動脈は，交感神経系と副交感神経系の両者の制御を受けており，副交感神経は太い血管の外膜のみに分布し，運動性および知覚性の神経線維を含む．交感神経は無髄運動神経線維を有し，細動脈レベルに至るまで分布し，中膜平滑筋細胞に入り込む．近位部の冠血管ではα交感神経刺激による血管収縮作用が優位で，遠位部の細血管では，α作用が消失していく．また，α交感神経受容体刺激による冠血管収縮作用の約70%が太い冠動脈の収縮により，残りの30%は冠抵抗血管に起因することが示されている．冠抵抗血管はβ交感神経のみならず，α交感神経活性による制御も受けており，互いが拮抗して冠血流量を調節している．さらに副交感神経刺激では，冠血管は拡張する．

d. 冠微小血管トーヌスの体液性調節

心筋組織でのpH，P_{O_2}が低下すれば冠血流量が増加

する．ATPの代謝産物であるアデノシンは，冠血流量の制御に重要な役割を果たしており（Horiら，1991），冠血管のアデノシンA_2受容体に作用し，冠血管平滑筋細胞内のcAMPレベルを増加させ，平滑筋を弛緩させる．アデノシンはおもに直径200μm以下の冠微小血管に作用して冠血管抵抗を低下させる．また，アデノシンは心筋酸素需要増大や心筋虚血の程度に応じて，反応性に冠血流量を増加させるのに十分な量が遊出され，冠血管に対して耐性が生じにくいとされる．一方，心筋虚血や低酸素により細胞内ATPレベルが低下するが，このATPレベル低下に呼応してK_{ATP}チャネルが開口する．冠血流量を低下させると直径100μm以下の冠微小血管が拡張するが，その作用はK_{ATP}チャネル遮断薬であるグリベンクラミドにて抑制されることが知られている．また，アセチルコリンなどが血管内皮細胞の受容体に結合することにより，Ca^{2+}の流入をもたらし，血管内皮細胞に局在する血管内皮型NO合成酵素（eNOS）を活性化して，NOを継続的に産生する．NOは直ちに血管平滑筋に取り込まれ，グアニル酸シクラーゼの活性化によりサイクリックGMP（cGMP）が産生され，cGMP依存性蛋白質リン酸化酵素の活性化を介して血管平滑筋を弛緩させる．これらアデノシン，K_{ATP}チャネル開口およびNOの三者が協調的に冠血流量調節に働いている．その他，内皮由来過分極因子（endothelium-derived hyperpolarizing factor; EDHF），PGI_2などもトーヌス調節に関与している．

(2) 心筋虚血の病態生理

a. 冠循環の変化による心筋収縮および拡張に及ぼす影響

心内膜下局所心筋短縮率または壁厚増加率が低下しはじめる臨界灌流圧（critical perfusion pressure）または自己調節能（autoregulation）の限界は，100 mmHgが正常血圧である麻酔犬では約70 mmHg，また覚醒犬では40 mmHgといわれている．冠動脈の近位部を結紮（けっさつ）すると，10秒後には灌流領域中心部の心筋短縮率が30%低下する．虚血がさらに持続すると心筋は収縮しなくなり，逆に収縮期を通じて伸展されるようになる．また，心筋虚血時には左室拡張機能障害を認める．拡張早期にみられる弛緩速度の低下と拡張中期から後期における拡張期スティフネス（コンプライアンスの逆数）の変化の2点である．心筋虚血が起こると収縮期よりも拡張期の指標の方が先に障害される．弛緩速度の低下の原因は，心筋虚血が起こるとATPの減少を認めるが，筋小胞体へのCa^{2+}の取り込みにはATPを要するため，収縮蛋白の不活性化が遅延するためと考えられている．拡張期スティフネスは，心筋虚血の状態では冠灌流圧が一定であれば冠血流量が増加するため，coronary turgorの増加（garden hose effect）や間質浮腫により増加し，冠血流遮断が1時間以上持続すると心筋のATPが枯渇してアクチン-ミオシン結合が解離できなくなり，不可逆性の虚血性拘縮のため著明に増加する．

b. 心筋虚血から心筋壊死巣への形成過程

心筋虚血による心筋壊死は心内膜側心筋より生じ，虚血時間が長くなるにつれて心外膜側心筋へと伝播する．イヌの実験モデルでは，冠動脈結紮後40分，3時間，96時間後の心筋梗塞巣の形成過程を検討したところ，15分以内の虚血では心筋壊死は生じなかったが，40分で心内膜側心筋に散在性に心筋壊死が生じた．さらに3時間後には，心内膜側心筋の壊死は完成し，96時間後には心筋壊死が心外膜側まで進行し貫壁性梗塞が完成する（wavefront現象）．wavefront現象を修飾する重要な因子としては，側副血流量や虚血プレコンディショニング現象，前負荷・後負荷，薬剤などが重要な因子である．実際，側副血行路の不良なブタでは冠動脈結紮後40分で心内膜側（1/3）に心筋壊死が生じ，1時間後には約80%，2時間で貫壁性梗塞が完成することが知られ，ヒトの心筋梗塞では，発症後3〜6時間以内に貫壁性梗塞が完成すると考えられている．

c. 心筋虚血における寄与因子

i) 側副血行路　側副血行路が発達しているイヌと側副血行路が乏しいブタを比較すると，心筋壊死形成に要する時間が異なることが知られていることから，側副血流量は心筋虚血から心筋梗塞に至る過程における重要な規定因子であると考えられる．イヌにおける検討では，冠動脈結紮後20分後の心筋外層・中層・内層への側副血流量はおのおの非虚血時の6，9，22%で，心内膜側により強い虚血障害が生じる．側副血行は，非虚血領域の心外膜側冠動脈の分枝により供給されるため，側副血管は心外膜側より心内膜側に穿通する．この側副血管は心筋内圧が高いために心内膜側を十分に灌流できないとされる．さらに，長時間持続による心筋虚血により不可逆性心筋障害が生じ，その周囲に出血・炎症・浮腫などが生じ側副血管を圧迫したり，トーヌス亢進を惹起するためと考えられる．

ii) 虚血プレコンディショニング　虚血プレコンディショニングとは，短時間心筋虚血の先行により，その後生じる長時間虚血による心筋細胞障害に対して保護的に作用する現象である．臨床において，心筋梗塞発症前に狭心症発作を有する急性心筋梗塞患者の予後や心機能が比較的良好であることが経験的に知られていた．その虚血改善効果のメカニズムとして，Murryらが，急性心筋梗塞モデルで実験的に同様の現象を明らかにした．そのことから，虚血プレコン

ディショニングは臓器保護の観点から普遍的な概念となった（Murry ら，1986）．プレコンディショニングには，心筋保護効果が 1～2 時間で消失する early phase プレコンディショニングと心筋保護効果が 24 時間～48 時間後に再び出現する late phase プレコンディショニングとがある．early phase プレコンディショニングのメカニズムは蛋白リン酸化が主に関与するのに対して，late phase プレコンディショニングは蛋白合成を伴った現象であると考えられている．プレコンディショニングの分子メカニズムは，early phase プレコンディショニングでは，アデノシンなどがプロテインキナーゼ C（PKC）活性化に続く ATP 感受性 K^+（K_{ATP}）チャネルを活性化させ心筋保護作用を惹起することによる．一方，late phase プレコンディショニングの分子メカニズムについては iNOS を介する NO 産生増加-HSP 72-MnSOD 連関および PKC-ecto-5′-nucleotidase 誘導-アデノシン連関の相加および相乗作用により惹起されるものと考えられている．このプレコンディショニング効果は，心筋梗塞サイズを縮小させるいちばん強い作用を有しており，現在臨床において，この作用に近い効果を有する薬剤の探索に力が注がれている．

d. 心筋スタニング（stunned myocardium）

実験的に冠動脈を短時間結紮した後，再灌流すると組織学的にほとんど異常がないにもかかわらず心筋収縮能の低下が数時間～数日持続する現象がある．この再灌流後の心筋収縮不全を，1982 年，Braunwald らが “stunned myocardium（気絶心筋）” と命名した．臨床においても，急性心筋梗塞患者において虚血・再灌流後，一時的な心筋収縮不全が認められることがわかってきた．虚血心における心筋収縮能の低下は心筋酸素消費量を低下させ，一見合目的な現象と考えられる．しかし stunned myocardium 時の局所の酸素消費量はむしろ増大しており，エネルギー代謝の面からも脂肪酸取り込み低下および糖取り込み亢進という非効率なエネルギー代謝があり，一種の再灌流障害とも考えられている．現在，心筋スタニングの原因として，①フリーラジカル発生，②心筋細胞内 Ca^{2+} 過負荷，の 2 つのメカニズムが考えられている（図 5-127）．1 つは，再灌流時に産生される O^{2-} や OH^- による細胞膜や膜上のイオンチャネル障害がスタニングの一因と考えられる．また，Ca^{2+} 過負荷がスタニングの原因とされることは，①低［Ca^{2+}］灌流液（または血液）で再灌流すると，スタニングは抑制される（低 Ca^{2+} 再灌流）こと，②徐々に灌流したり，酸性溶液添加によりアシドーシスの回復を緩徐にすると，スタニングが抑制される（段階的再灌流，酸性再灌流）こと，③細胞外液の Ca^{2+} レベルを上昇させると，一過性には陽性変力作用を示すが，これを繰り返すと発生張力が低下することより，Ca^{2+} 過負荷により心筋陽性変力作用の Ca^{2+} 感受性が低下することから支持されている（図 5-128）．しかしながら，なぜ Ca^{2+} 過負荷がスタニングを惹起するのかは明らかでない．細胞骨格蛋白であるマイクロチュブルが障害をうけ，その障害程度が心機能低下と相関することから，細胞骨格の障害がスタニングの一因となっていることが考えられている．Ca^{2+} が結合することにより，アクチン-ミオシンのスライディングが生じるトロポニン C の障害が生じることが報告されており，Ca^{2+} に関係した収縮蛋白の障害が関与するものと思われる．

e. ハイバネーション（冬眠心筋，myocardial hibernation，hibernating myocardium）

心筋ハイバネーションは，冠血流量が低下しても心筋は酸素供給に見合うように心機能を低下させ虚血性

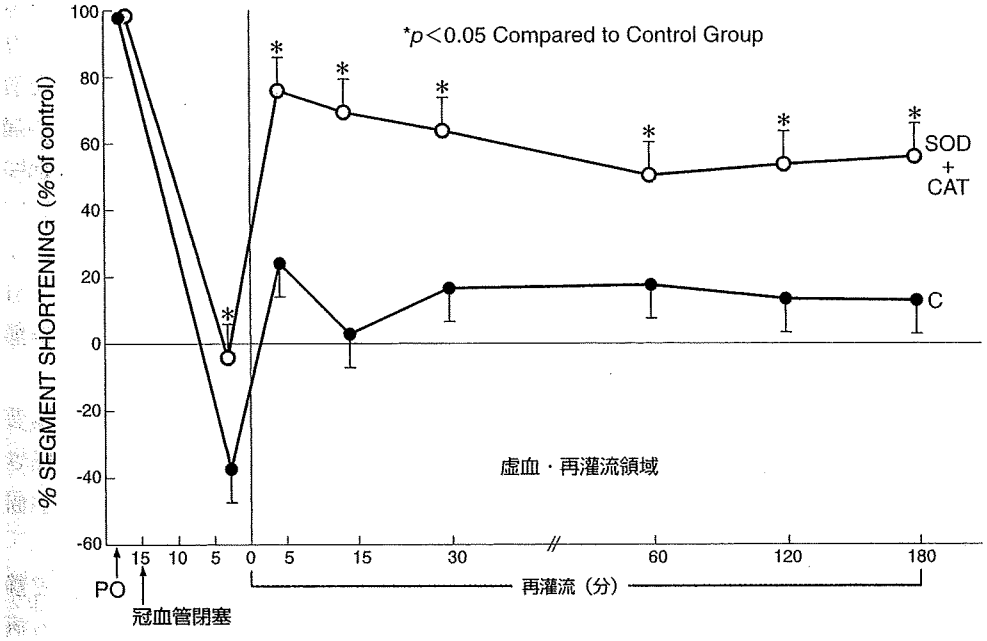

〈図 5-127〉虚血・再灌流領域における心筋短縮率
15 分虚血刺激後の心筋短縮率低下（赤線）は SOD＋カタラーゼ投与（青線）により抑制される（Gross ら，1986）．

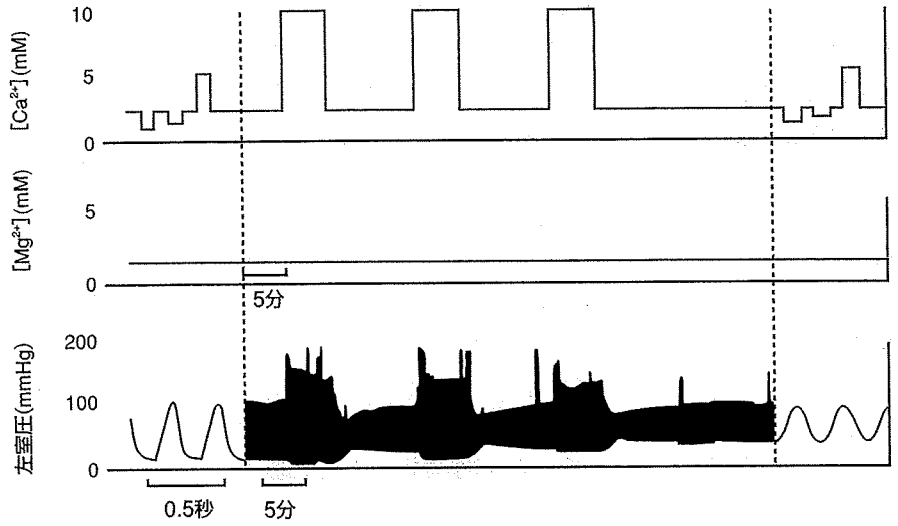

〈図 5-128〉一過性 Ca^{2+} 過負荷の左室発生圧に及ぼす影響
Ferret の Langendorff 心標本において，細胞外 Ca^{2+} を一過性に増加させると，左室発生圧は低下する（Kitakaze ら，1988）．

代謝変化を呈さない状態をいう．この概念は臨床的に，冠動脈狭窄のある患者が冠動脈バイパス術をうけた後，心機能の改善がみられることから提唱されたものである．臨床的に左室造影，心エコー・核医学検査でアキネジアや運動障害を示した領域の 7% に，また運動低下を示した領域の 52% に剖検で正常心筋組織が含まれていることから，壊死に陥っていない心筋にも収縮能低下が認められることは確かである．一方，冠血行再建術により心機能の改善がみられ ^{201}Tl 心筋シンチグラム像でも欠損が消失する症例が少なくない．ブタの冠動脈を 80% 狭窄すると，5 分で冠静脈血の pH は低下し局所心筋短縮率も減少し明らかな虚血変化を呈するが，40 分後には収縮性の低下は存在するにもかかわらず，乳酸産生および冠静脈血 pH は回復する．このような低灌流に対する適応のメカニズムは明確でないが，低灌流圧や冠血流量に依存して心収縮性が変化する Gregg 現象が一因と考えられている．PET でハイバネーション心筋を観察すると ^{201}Tl の局所取り込みは低下し局所血流が少ないにもかかわらず，糖（FDG）の取り込みは上昇している．したがって，解糖系による ATP 産生は亢進しており，ハイバネーションは，心筋代謝が虚血状態に適応している可能性が高い．しかし，一方で心筋ハイバネーションには繰り返す心筋虚血が関与しているとする考え方もある．慢性冠動脈疾患の患者の Holter 心電図解析により，無症候性心筋虚血が高頻度に生じていることがわかっている．Rahimtoola らは，心筋ハイバネーションを「安静時には無症候であるが可逆的な心筋虚血が持続している左心室機能異常である」との仮説を唱えている．したがって，心筋ハイバネーションは種々の虚血状態よりなる病態である可能性がある．

〔朝倉正紀・浅沼博司・北風政史〕

■文　献
Gross GJ, Farber NE, et al: Beneficial actions of superoxide dismutase and catalase in stunned myocardium of dogs. *Am J Physiol*, 250: H 372-377, 1986.
Hori M, Kitakaze M: Adenosine, the heart, and coronary circulation. *Hypertension*, 18: 565-574, 1991.
Kitakaze M, et al: Contractile dysfunction and ATP depletion after transient calcium overload in perfused ferret hearts. *Circulation*, 77: 685-695, 1988.
Murry CE, Jennings RB, et al: Preconditioning with ischemia: a delay of lethal cell injury in ischemic myocardium. *Circulation*, 74: 1124-1136, 1986.

2）狭心症
angina pectoris

【定義・概念】

狭心症は一過性の心筋虚血（酸素不足）の結果，特有の胸痛発作（狭心痛），心電図変化，心筋代謝異常，心機能障害をきたす臨床症候群である．高度の貧血や大動脈弁膜症などの心筋に酸素不足をもたらす病態も狭心症の原因となるが，一般には冠動脈の異常により生じた虚血発作を狭心症とよぶ．心筋梗塞の既往を有する例も少なくない．なお心筋虚血があっても狭心痛を認めないこともしばしばある［無症候性心筋虚血⇨5-6-3）参照］．

【分　類】

病態（発症機序），発作の誘因，経過の観点から分類されるが（表 5-42），治療を考えるうえでは病態をどうとらえるかが最も重要である．

1）病態よりみた分類：　器質的冠狭窄による器質性狭心症，冠攣縮（れんしゅく）性狭心症，急性冠症候群に分類される．冠動脈造影所見に基づいて診断されるが，症候から推定することも可能である（後述）．

2）発作の誘因よりみた分類：　労作狭心症，安静狭心症，労作兼安静狭心症に分類される．必ずしも病

態を反映せず，たとえば労作狭心症であっても器質的冠狭窄によることもあれば，労作により誘発された冠攣縮によることもある．

3) 経過よりみた分類： 安定狭心症，不安定狭心症に分類される．安定狭心症はある一定以上の労作にて生じる安定労作狭心症を意味する．一方，不安定狭心症は急性心筋梗塞（AMI）や突然死に至る可能性のある重症の狭心症で，表5-43のように細分類される．不安定狭心症の多くは急性心筋梗塞と同様の病態（後述）で発症するため，急性心筋梗塞とともに急性冠症候群ともよばれる．

【原因・病因】

動脈硬化を原因とし，以下の危険因子が動脈硬化の進展を助長する．

1) 冠危険因子： 制御不可能な因子として，年齢，性（男性），家族歴，人種があげられる．男性45歳以上，女性55歳以上が危険因子とみなされる．制御可能な因子としては，高脂血症，高血圧，糖尿病，肥満，高尿酸血症などがあげられるが，これらも遺伝的素因に基づくところが大きい．

〈表5-42〉狭心症の分類

1. 病態（発症機序）の観点より
   - 器質性狭心症
   - 冠攣縮性狭心症（異型狭心症）
   - 急性冠症候群
2. 発作の誘因の観点より
   - 労作狭心症
   - 安静狭心症
   - 労作兼安静狭心症
3. 経過の観点より
   - 安定狭心症
   - 不安定狭心症

〈表5-43〉不安定狭心症の分類

1. ISFC/WHO*1の分類（1979年）
   - a. 新規労作狭心症
   - b. 増悪型労作狭心症
   - c. 自発性狭心症（安静狭心症）
2. Canadian Cardiovascular Societyの分類（1976年）
   - a. 1週間以内に発症した安静狭心症
   - b. 2カ月以内に発症したCCSC*2 3-4度の新規狭心症（表5-44参照）
   - c. CCSC 3-4度の増悪型狭心症
   - d. 異型狭心症
   - e. 非Q波心筋梗塞症
   - f. 発症24時間以降の梗塞後狭心症
3. Braunwaldの重症度分類（1989年）
   - class Ⅰ
     - a. 最近の2カ月以内に発症した重症の初発労作狭心症
     - b. 1日に3回以上発作が頻発するか，わずかな労作にても発作が起きる増悪型労作狭心症．安静狭心症は認めない．
   - class Ⅱ
     最近の1カ月以内に発症した安静狭心症で，48時間以内に発作のないもの（亜急性型）
   - class Ⅲ
     48時間以内に発作を認めた安静狭心症（急性型）

*1 ISFC/WHO : International Society and Federation of Cardiology/World Health Organization.
*2 CCSC : Canadian Cardiovascular Society Criteria.

2) 生活習慣様式： 喫煙，職業（ストレス），性格が動脈硬化の進展と関連する．カロリー摂取過多と脂質の過剰摂取，そして運動不足はともに肥満，耐糖能異常の大きな原因となり，特に不安定プラークの発生を助長する［⇨13-5参照］．

【疫学・発生率】

米国における年間発生率は年齢30歳以上の10万人あたり213例とされる．わが国における正確な発生率は不明であるが，1992年の厚生労働省の主要傷病別患者調査によると虚血性心疾患患者総数は91万1000人であった．このなかには心筋梗塞や胸痛症候群も一部含まれるが，心筋梗塞例でも狭心症をしばしば認めるため，狭心症の年間発生数は相当数に達するものと考えられる．男性が3～6倍多いとされ，年齢は男性では45歳以上，女性では55歳以上が多い．

【病態生理および症候との関連】

心筋虚血が発生する機序として，心筋の酸素需要の増大に酸素供給が追いつかなくなる場合（相対的酸素不足）と，酸素供給自体が減少する場合（絶対的酸素不足）があげられる（図5-129）．前者は器質的冠狭窄を，後者は冠攣縮や血栓を原因とする［⇨詳細は5-6-1）参照］．

1) 器質的冠狭窄（器質性狭心症）： 動脈硬化プラークにより内膜が肥厚し，冠動脈内腔の狭窄をきたして冠血流量の増加が制限されやすくなる．特に労作時などの心筋酸素需要の増大に応じた酸素供給が困難になって心筋が虚血に陥り狭心症が発症する．一般に断面積で50%以上（内径で70%以上）の狭窄があると冠血流が制限され（有意狭窄病変），80～90%以上の狭窄があると安静時の心筋酸素需要にも応じきれなくなり，ほかの冠動脈枝からの側副血行が発達するとされる．

症候との関連：冠動脈の1枝に高度狭窄病変を有する1枝病変例では強度の労作時のみに狭心症を認める（安定労作狭心症）．一方，2枝以上の多枝に高度狭窄病変を有する多枝病変例では，側副血行も制限されるため容易に広範囲の心筋に虚血を生じ，軽度の労作でも狭心症発作を生じる（増悪型狭心症）．1枝

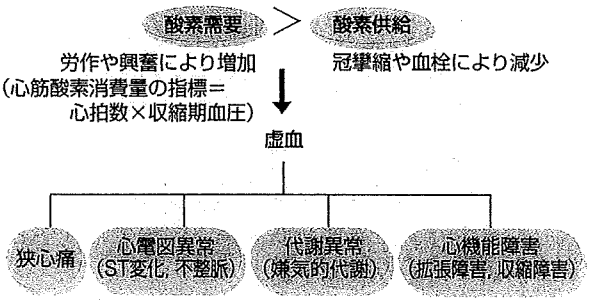

〈図5-129〉心筋虚血の病態生理

Cardiovascular Research (2008) 79, 600–610
doi:10.1093/cvr/cvn128

Overexpression of endoplasmic reticulum-resident chaperone attenuates cardiomyocyte death induced by proteasome inhibition

Hai Ying Fu[1], Tetsuo Minamino[2]*, Osamu Tsukamoto[2], Tamaki Sawada[2], Mitsutoshi Asai[2], Hisakazu Kato[2], Yoshihiro Asano[2], Masashi Fujita[2], Seiji Takashima[2], Masatsugu Hori[2], and Masafumi Kitakaze[1]

[1]*Department of Cardiovascular Medicine, National Cardiovascular Center, Suita, Osaka 565-8565, Japan; and* [2]*Department of Cardiovascular Medicine, Osaka University Graduate School of Medicine, 2-2 Yamadaoka, Suita, Osaka 565-0871, Japan*

Received 17 December 2007; revised 8 April 2008; accepted 13 May 2008; online publish-ahead-of-print 28 May 2008

Time for primary review: 28 days

KEYWORDS
ER stress;
CHOP;
GRP78;
Proteasome inhibition;
Cardiomyocyte

Aims Proteasome inhibitors are a novel class of anticancer agents that induce tumour cell death via endoplasmic reticulum (ER) stress. Since ER stress is involved in the development of heart failure, we investigated the role of ER-initiated cardiomyocyte death by proteasome inhibition.

Methods and results Rat neonatal cardiomyocytes were used in this study. Proteasome activity was assayed using proteasome peptidase substrates. Cell viability and apoptosis were measured by 3-(4,5-dimethylthiazol-2-yl)-2,5-diphenol tetrazolium bromide and flow cytometry, respectively. Western blot analysis, real-time polymerase chain reaction (PCR) and reverse transcriptional PCR were used to detect the expression of protein and messenger ribonucleic acid (RNA). The location of overexpressed glucose-regulated protein (GRP) 78 was observed by confocal fluorescence microscopy. Proteasome inhibition induced cardiomyocyte death and activated ER stress-induced transcriptional factor ATF6, but not XBP1 (X-box binding protein 1), without up-regulating ER chaperones. ER-initiated apoptosis signalling, including cytosine-cytosine-adenine-adenine-thymine enhancer-binding protein (C/EBP) homologous protein (CHOP), c-Jun-N-terminal kinase (JNK), and caspase-12, was activated by proteasome inhibition. Short interference RNA targeting CHOP, but not the blockage of caspase-12 or JNK pathway, attenuated cardiomyocyte death. Overexpression of GRP78 suppressed both CHOP expression and cardiomyocyte death by proteasome inhibition.

Conclusion These findings demonstrate that proteasome inhibition induces ER-initiated cardiomyocyte death via CHOP-dependent pathways without compensatory up-regulation of ER chaperones. Supplement and/or pharmacological induction of GRP78 can attenuate cardiac damage by proteasome inhibition.

1. Introduction

Endoplasmic reticulum (ER) is an organelle that participates in the folding of membrane and secretory proteins. The conditions or stresses that interfere with ER function are named ER stress.[1] There are two ER stress-induced transcriptional factors to up-regulate ER-resident chaperones that promote the folding of accumulated proteins in ER: activating transcription factor 6 (ATF6) and X-box binding protein 1 (XBP1). ATF6 is cleaved in response to ER stress and the cleaved ATF6 traffics to nuclei to induce the expression of ER-resident chaperone.[2] In addition, ER stress induces *XBP1* messenger ribonucleic acid (mRNA) splicing, producing a new spliced *XBP1* mRNA.[3] The spliced XBP1 protein and cleaved ATF6 cooperatively up-regulate the expression of ER-resident chaperones that reduce ER stress.[4] Another important pathway to cope with ER stress is the degradation of misfolded proteins by the ubiquitin-proteasome system.[5] It is therefore conceivable that treatment of cells with proteasome inhibitors causes accumulation of misfolded proteins and ER stress. When the overload of misfolded proteins is not resolved, cell apoptosis signals are initiated from ER. This effect is mediated by increased expression of the transcription factor cytosine-cytosine-adenine-adenine-thymine enhancer-binding protein (C/EBP) homologous protein (CHOP) and activation of caspase-12 and c-Jun-N-terminal kinase (JNK).[6–8]

Recently, the ubiquitin-proteasome system is reported to be involved in the growth and survival of cells and

* Corresponding author. Tel: +81 6 6879 3472; fax: +81 6 6879 3473.
E-mail address: minamino@medone.med.osaka-u.ac.jp

considered as an attractive therapeutic target.[9] Proteasome inhibitors are usually short peptides linked to a pharmacophore that reacts with the active site of proteasome.[10] Based on the pharmacophores, proteasome inhibitors can be divided into several groups: peptide aldehydes (e.g. MG132), peptide boronates (e.g. PS341), and peptide epooxyketones (e.g. epoxomicin).[11] Among these proteasome inhibitors, bortezomib (PS341) has been used as anticancer agent against haematological malignancy and solid tumours.[12] Recently, the treatment with bortezomib was reported to be associated with cardiac failure in patients with lung cancer and multiple myeloma.[13,14] Furthermore, we have found that the accumulation of ubiquitinated proteins in failing heart samples from humans demonstrated the impairment of proteasome function in failing hearts.[15] These findings led us to hypothesize that the proteasome inhibition could cause cardiomyocyte death via an ER-dependent pathway. To test this hypothesis, we checked the role of ER-initiated apoptotic signalling in cardiomyocyte death when proteasome activity was pharmacologically inhibited. Furthermore, we also investigated whether overexpression of ER-resident chaperone could rescue cardiac cell death by proteasome inhibition. In the present study, we used MG132 and epoxomicin, two typical proteasome inhibitors, to investigate the effect of proteasome inhibition on cardiomyocytes. We also used tunicamycin, an inhibitor of N-linked glycosylation, as an ER stress inducer without affecting proteasome activity.

2. Methods

2.1 Materials

MG132, epoxomicin, and tunicamycin were purchased from Sigma Chemical Co. (St Louis, MO, USA). The antibodies for CHOP, XBP1, ATF6, and actin were obtained from Santa Cruz Biotechnology (Santa Cruz, CA, USA). The antibodies for phospho-JNK and JNK were obtained from Cell Signaling Technology, Inc. (Danvers, MA, USA). The antibodies for caspase-12 and HP1α were obtained from Sigma Chemical Co., while those for Lys-Asp-Glu-Leu (KDEL) and glyceraldehyde-3-phosphate dehydrogenase (GAPDH) were obtained from Assay Designs, Inc. (Ann Arbor, MI, USA) and Millipore Co. (Billerica, MA, USA). Z-Ala-Thr-Ala-Asp (Z-ATAD) and SP600125 were purchased from BioVision Inc. (Mountain View, CA, USA) and Calbiochem (San Diego, CA, USA), respectively.

2.2 Preparation of neonatal rat cardiomyocytes

Primary cardiomyocyte cultures were prepared from neonatal rat hearts as described previously.[16] All procedures were in accordance with the guiding principles of Osaka University School of Medicine, Position of the American Heart Association on Research Animal Use, and the Guide for the Care and Use of Laboratory Animals published by the US National Institute of Health (NIH Publication No. 85-23, revised 1996).

2.3 Proteasome activity assay

Chymotrypsin-like activities of proteasome were assayed using the fluorogenic peptides Suc-Leu-Leu-Val-Tyr-7-amino-4-methylcoumarin (LLVY-AMC) (Biomol, Plymouth Meeting, PA, USA) according to the method reported previously.[15] Briefly, after the treatment with MG132 or epoxomicin for 30 min, cultured rat neonatal cardiomyocytes were harvested, lysed in proteasome buffer (10 mmol/L Tris–HCl, pH 7.5, 1 mmol/L ethylene diamine tetraacetic acid (EDTA), 2 mmol/L adenosine-5'-triphosphate, 20% glycerol, and 4 mmol/L dithiothreitol), and centrifuged at 13 000 g at 4°C for 10 min. Then the supernatant (20 μg of protein) was incubated with proteasome activity assay buffer (0.05 mol/L Tris–HCl, pH 8.0, 0.5 mmol/L EDTA, 40 μmol/L LLVY-AMC) for 1 h at 37°C. The reaction was stopped by adding 0.9 mL of cold water and placing the reaction mixture on ice for at least 10 min. Subsequently, the fluorescence of the solution was measured by Fluorescence Microplate Reader (Gemini XS; Molecular Devices, Sunnyvale, CA, USA) with excitation at 380 nm (Ex) and emission at 440 nm (Em). All readings were standardized relative to the fluorescence intensity of an equal volume of free 7-amino-4-methylcoumarin (Sigma) solution (40 μmol/L).

2.4 Caspase-12 activity assay

Caspase-12 activity was assayed using its substrate ATAD-7-amino-4-trifluoromethyl coumarin. Cell lysate aliquots were assayed by Fluorescence Microplate Reader (Gemini XS; Molecular Devices) with 400 nm excitation and 505 nm emission filter according to the manufacturer's protocol (BioVision).

2.5 3-(4,5-Dimethylthiazol-2-yl)-2,5-diphenol tetrazolium bromide assay

Cardiomyocytes were seeded at 3×10^4/well in 96-well plates. After MG132 administration at appropriate conditions, cell numbers were measured with a water-soluble tetrazolium reagent [WST-8; 2-(2-methoxy-4-nitrophenyl)-3-(4-nitrophenyl)-5-(2,4-disulfophenyl)-2H-tetrazolium, monosodium salt] (Dojindo Laboratories, Kumamoto, Japan) according to the manufacturer's instructions. Cell viability was expressed as a percentage of the control. The wavelengths used in this assay were 450 nm (sample) and 630 nm (reference).

2.6 Western blot analysis

Cardiomyocytes were lysed in the buffer (0.15 mmol/L, NaCl 0.05 mmol/L Tris–HCl, pH 7.2, 1% Triton X-100, 1% sodium deoxycholate, 0.1% SDS) containing a protease inhibitor cocktail (Nakarai Tesque, Kyoto, Japan). Electrophoresis, immunoblotting, and detection were done as described previously.[15]

2.7 Reverse transcriptional polymerase chain reaction

After rat cardiomyocytes were treated with the drugs for 6 h, *XBP1* mRNA splicing was assessed using reverse transcriptional polymerase chain reaction (PCR) method. The primers that spanned the splice site are designed as followed: forward, ACGAGAGAAAACTCATGG; reverse, ACAGGGTCCAACTTGTCC (*Figure 1D*). This pair of primers can detect both spliced and unspliced *XBP1* at the size of 290 and 264 bp, respectively. The primers for GAPDH are forward, CATCAACGACCCCTTCATTGACCTCAACTA;reverse,TCCACGATGCCAAAGTTGTCATGGATGACC. PCR products were resolved on a 2% agarose gel and viewed by UV illumination.

2.8 Real-time quantitative polymerase chain reaction

We obtained samples after the drug treatment and then they were prepared according to the Omniscript Reverse Transcription Handbook (QIAGEN Inc., Hilden, Germany). The rat primers and probes used for quantification of glucose-regulated protein (GRP) 78, GRP94, CHOP, and GAPDH were all designed according to the manufacturer's protocol (Applied Biosystems, Foster City, CA, USA. https://www.appliedbiosystems.com/). Real-time PCR was performed with an ABI PRISM 7000 Sequence Detection System

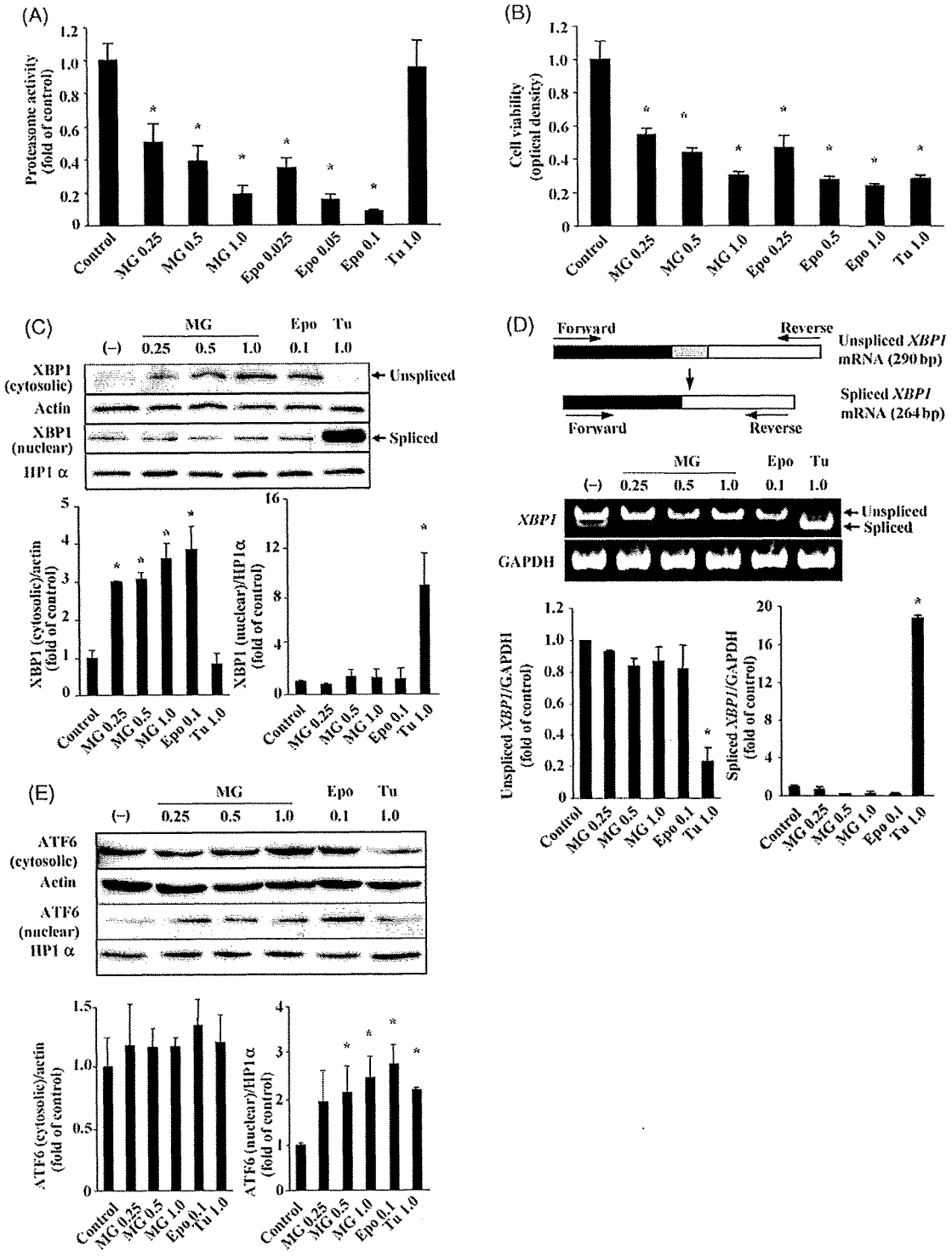

Figure 1 Effects of pharmacological proteasome inhibitors on the proteasome activity, cell death and endoplasmic reticulum stress-induced transcriptional factors in cultured cardiomyocytes. (*A*) Proteasome activity after the treatment with MG132 (MG) (0.25, 0.5, 1.0 μmol/L), epoxomicin (Epo) (0.025, 0.05, 0.1 μmol/L) or tunicamycin (Tu) (1.0 mg/mL) for 30 min. Experiments were repeated independently for three times ($n = 3$ in each experiment). (*B*) Cardiomyocyte viability after the treatment with MG, Epo or Tu for 48 h. Experiments were repeated independently for four times ($n = 6$ in each experiment). (*C*) Western blot analysis of spliced and unspliced X-box binding protein 1 (XBP1) proteins after the treatment with MG (0.25, 0.5, 1.0 μmol/L), Epo (0.1 μmol/L) or Tu (1.0 μg/mL) for 6 h. Actin and HP1α were used as the internal controls of cytosolic and nuclear fractions, respectively. (*D*) The upper panel shows the design of polymerase chain reaction (PCR) primers for *XBP1* messenger ribonucleic acid (mRNA) used in this study. This pair of primers can detect both unspliced and spliced *XBP1* mRNA. The middle and lower panels are representative and quantitative results of reverse transcriptional PCR for spliced and unspliced *XBP1* mRNA after the treatment with MG (0.25, 0.5, 1.0 μmol/L), Epo (0.1 μmol/L) or Tu (1.0 μg/mL) for 6 h. Glyceraldehyde-3-phosphate dehydrogenase was used as the internal control of mRNA expression. (*E*) Western blot analysis of ATF6 (activating transcription factor 6) in cytosolic and nuclear fractions after the treatment with MG (0.25, 0.5, 1.0 μmol/L), Epo (0.1 μmol/L) or Tu (1.0 μg/mL) for 6 h. The quantitative data in *C*, *D*, and *E* were achieved from three independent experiments. (Asterisk) $P < 0.05$ vs. control.

(Applied Biosystems) by the relative standard curve method. The thermal cycle reaction was performed as follows: 50°C for 2 min, 95°C for 10 min followed by 40 cycles at 95°C for 15 s, 60°C for 1 min. The target amount was determined from the relative standard curves constructed with serial dilutions of the control total cDNA.

2.9 Ribonucleic acid interference

We ordered four different short interfering ribonucleic acid (siRNA) from B-Bridge International, Inc. (Mountain View, CA, USA) to knock down CHOP mRNA (CHOP siRNA-1: 5′-CGAAGAGGAAGAAUCAAA-3′, siRNA-2: 5′-GGAAACAGCGACUGAAGGA-3′, siRNA-3: 5′-GGGACUGA GGGUAGACCAA-3′, siRNA-4: cocktail containing equal amounts of the above three types of siRNA). Rat cardiomyocytes were isolated and then incubated in Dulbecco's modified Eagle's medium (Invitrogen Co., Carlsbad, CA, USA). Opti-MEM (Invitrogen Co.), siRNA oligonucleotides (CHOP siRNA 1–4) (60 nmol/L) and Optifect (Invitrogen Co.) were added 4 h after cardiomyocyte isolation. As a negative control, cells were transfected with siRNA against firefly luciferase from Photinus pyralis (GL2 siRNA).

2.10 Flow cytometry

An Annexin V-fluorescein isothiocyanate (FITC) Apoptosis Detection Kit was purchased from Sigma. After the treatment of MG132, cardiomyocytes were washed twice with PBS and resuspended in binding buffer. FITC-Annexin V and propidium iodide were added according to the manufacturer's protocol. The mixture was incubated for 10 min in dark at room temperature and then cellular fluorescence was measured with a FACSscan flow cytometry (Becton, Dickinson and Company, Franklin Lakes, NJ, USA).

2.11 Adenovirus transduction

Recombinant adenovirus harbouring GRP78 gene was constructed as described previously,[17] and adenovirus harbouring LacZ was used as a control. Adenovirus was transfected 24 h after cardiomyocytes were isolated or 20 h after siRNA against CHOP was added. And the experiments were performed another 24 h after adenovirus infection.

2.12 Confocal fluorescence microscopy

Cardiomyocytes were observed by confocal microscopy (Radiance 2100 Laser Scanning System Bio-Rad, Hemei Hempstead, UK) and saved by LaserSharp 2000 (Bio-Rad). Alexa568 (red) (Invitrogen Co.) was scanned by helium/neon laser (wavelength 543 nm laser line) with long path 590 filter (560–700 nm excitation). Alexa488 (green) was captured by Argon laser (wavelength 488 nm laser line) with band path 500–550 IR filter (500–550 nm excitation). DAPI (blue) for nuclei staining of all cells was obtained in range of 400–470 nm excitation.

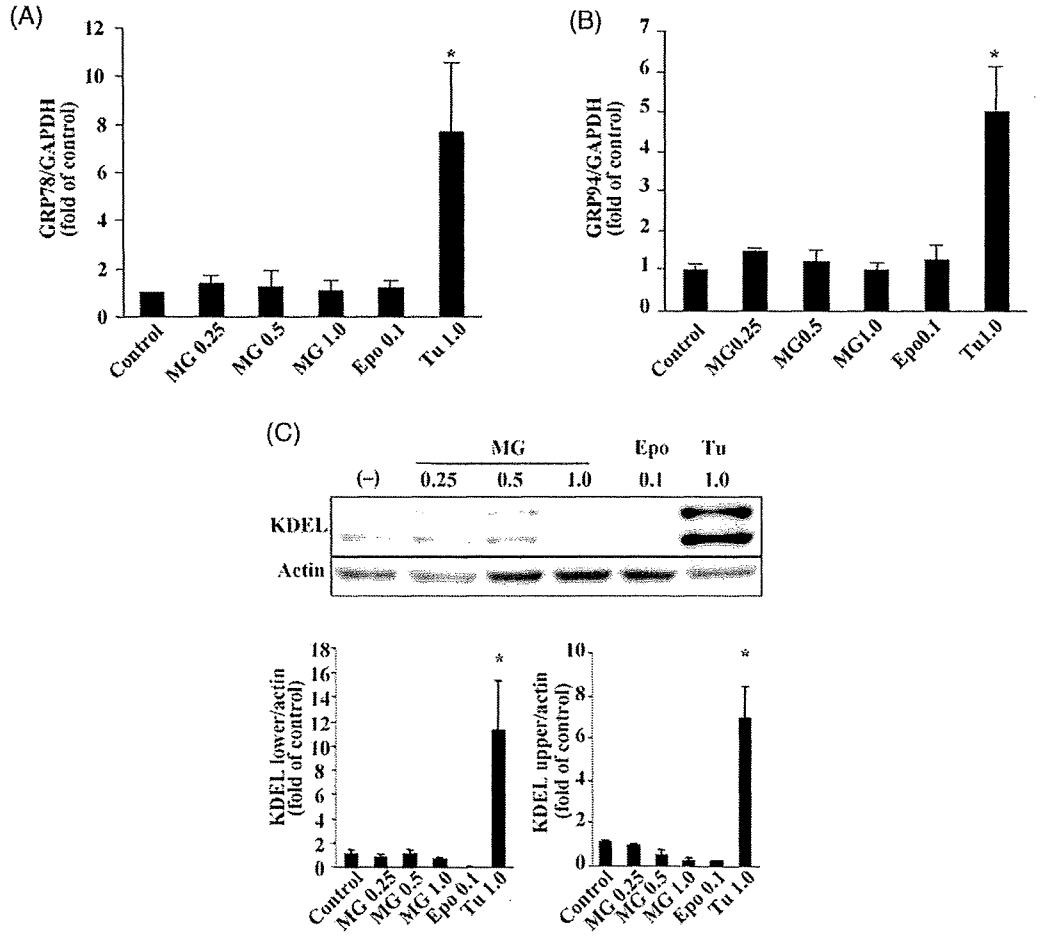

Figure 2 Endoplasmic reticulum chaperon expression by proteasome inhibition in cultured cardiomyocytes. Real-time polymerase chain reaction analysis of glucose-regulated protein (GRP) 78 (*A*) and GRP94 (*B*) ($n = 3$ in each experiment) and western blot analysis of Lys-Asp-Glu-Leu (KDEL) proteins (*C*) (upper and lower bands indicate GRP94 and GRP78, respectively) after the treatment with MG132 (MG) (0.25, 0.5, 1.0 μmol/L), epoxomicin (Epo) (0.1 μmol/L) or tunicamycin (Tu) (1.0 μg/mL) for 6 h. The western blot analysis and real-time PCR experiment were repeated for three times independently. (Asterisk) $P < 0.05$ vs. control.

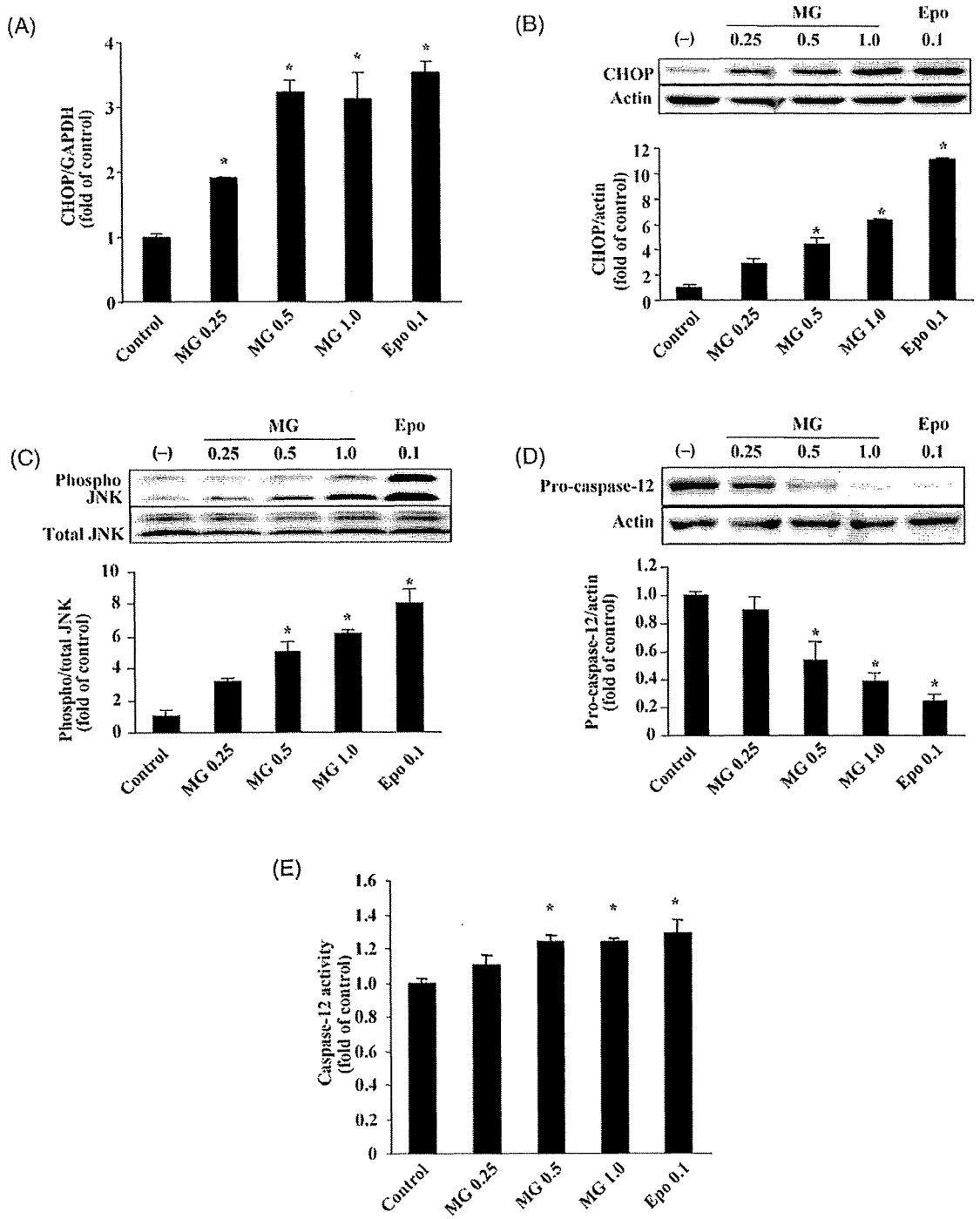

Figure 3 Activation of endoplasmic reticulum-initiated apoptosis signalling by proteasome inhibition in cultured cardiomyocytes. Real-time polymerase chain reaction (*A*) ($n = 3$ in each experiment) and western blot (*B*) analysis of CHOP [cytosine-cytosine-adenine-adenine-thymine (CCAAT) enhancer-binding protein (C/EBP) homologous protein] after the treatment with MG132 (MG) (0.25, 0.5, 1.0 μmol/L) or epoxomicin (Epo) (0.1 μmol/L) for 6 h. Western blot analysis of phospho-c-Jun-N-terminal kinase (JNK) (*C*) and pro-caspase-12 (*D*) after the treatment with MG (0.25, 0.5, 1.0 μmol/L) or Epo (0.1 μmol/L) for 1 and 6 h, respectively. (*E*) Caspase-12 activity after the treatment with MG (0.25, 0.5, 1.0 μmol/L) or Epo (0.1 μmol/L) for 6 h in cultured cardiomyocytes. Experiments were repeated independently for three times ($n = 3$ in each experiment). The quantitative data were achieved from three independent experiments. (Asterisk) $P < 0.05$ vs. control.

2.13 Statistical analysis

Data are expressed as the mean ± SEM. The results of cardiac proteasome activity, caspase-12 activity, cell viability and quantitative analysis of western blot analysis, real-time PCR, reverse transcription-PCR, and flow cytometry were compared by one-way factorial ANOVA followed by Bonferroni's correction. For all analyses, $P < 0.05$ was accepted as statistically significant.

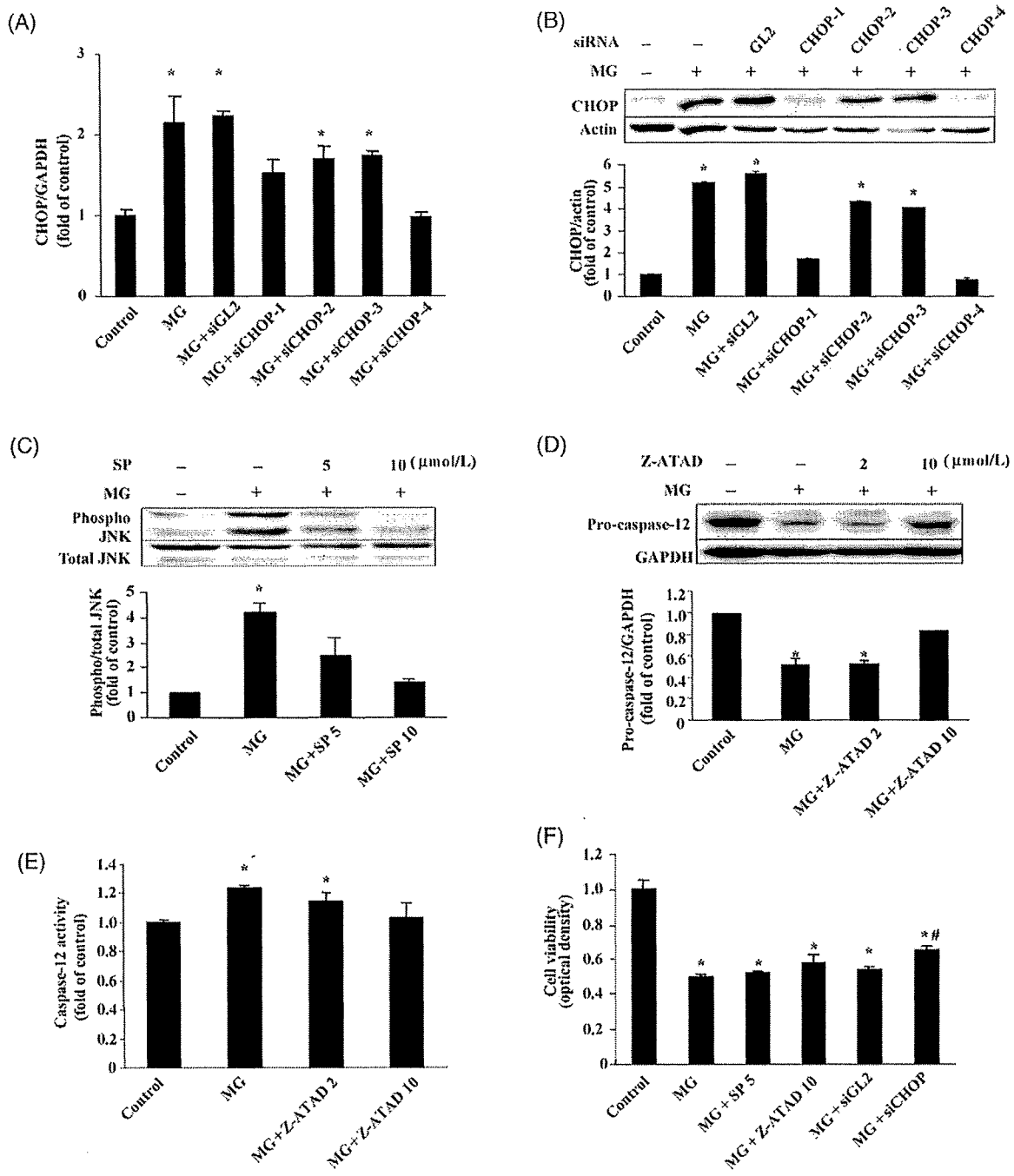

Figure 4 Effects of blockade of endoplasmic reticulum (ER)-initiated apoptosis signalling on apoptosis by proteasome inhibition in cultured cardiomyocytes. Effects of four different types of siRNA (short interfering ribonucleic acid) targeting CHOP [CCAAT enhancer-binding protein (C/EBP) homologous protein] on *CHOP* mRNA (*A*) ($n = 3$ in each experiment) and protein expression (*B*) after the treatment with MG132 (MG) (1.0 μmol/L) for 6 h. (*C*) Effects of SP600125 on JNK (c-Jun-N-terminal kinase) phosphorylation after the treatment with MG (1.0 μmol/L) for 1 h. SP600125 was added 1 h before MG (1.0 μmol/L) administration. (*D*) and (*E*) Effects of Z-Ala-Thr-Ala-Asp (Z-ATAD) on caspase-12 activation after the treatment with MG (1.0 μmol/L) for 6 h. Z-ATAD was added 1 h before MG (1.0 μmol/L) administration ($n = 3$ in each experiment). (*F*) Results of cardiomyocyte viability by MTT [3-(4,5-dimethylthiazol-2-yl)-2,5-diphenol tetrazolium bromide] assay after the co-treatment with MG (1.0 μmol/L) and blockers of ER-initiated apoptosis signals ($n = 6$ in each experiment). Representative (*G*) and quantitative (*H*) data of cardiomyocyte apoptosis by flow cytometry ($n = 3$ in each experiment). The population of cells in the lower right quadrant of dot plot indicated apoptotic cardiomyocytes. Results of western blot and flow cytometry analysis represented three independent experiments, while the result of cell viability was from four independent experiments, respectively. (Asterisk) $P < 0.05$ vs. control; (Hash) $P < 0.05$ vs. MG (1.0 μmol/L).

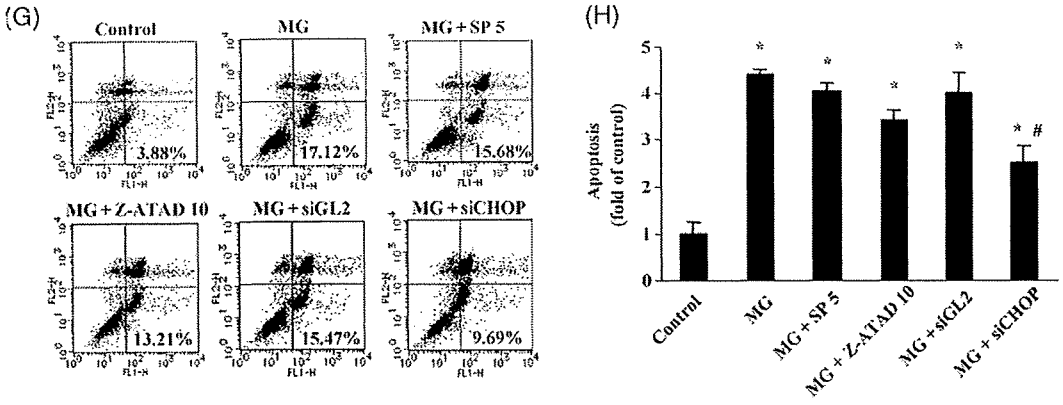

Figure 4 Continued.

3. Results

3.1 Proteasome activity and cell death by proteasome inhibition in cultured cardiomyocytes

Pharmacological proteasome inhibitors such as MG132 or epoxomicin dose-dependently decreased proteasome activity and reduced cell viability in rat-cultured cardiomyocytes. However, tunicamycin, an ER-stress inducer, induced cardiomyocyte death without inhibiting proteasome activity (*Figure 1A* and *B*).

3.2 Activation of endoplasmic reticulum stress-induced transcriptional factors and endoplasmic reticulum chaperone expression by proteasome inhibition in cultured cardiomyocytes

After the addition of MG132 or epoxomicin, protein level of unspliced XBP1 in cytosolic fraction, but not spliced XBP1 in nuclear fraction, was increased in rat-cultured cardiomyocytes (*Figure 1C*). The result of reverse transcriptional PCR demonstrated that either MG132 or epoxomicin did not change mRNA level of unspliced *XBP1* in cardiomyocytes (*Figure 1D*), suggesting that the increase in unspliced XBP1 protein level was due to the inhibition of its degradation by proteasome inhibition. In contrast, pharmacological ER stressor, tunicamycin, decreased unspliced *XBP1* mRNA expression and increased both mRNA and protein levels of spliced *XBP1* (*Figure 1C* and *D*). Proteasome inhibitors increased the protein level of ATF6 in the nuclear fraction in cultured cardiomyocytes (*Figure 1E*) to the similar extent as tunicamycin did. Importantly, proteasome inhibition did not induce the mRNA and protein expressions of either GRP78 or GRP94, although tunicamycin increased both of them (*Figure 2A–C*).

3.3 Activation of endoplasmic reticulum-initiated apoptosis signalling and cell death by proteasome inhibition in cultured cardiomyocytes

Proteasome inhibition by MG132 or epoxomicin increased both mRNA and protein levels of CHOP in rat-cultured cardiomyocytes (*Figure 3A* and *B*). In addition, it also induced JNK phosphorylation (*Figure 3C*) and caspase-12 activation (*Figure 3D* and *E*). CHOP siRNA 1 or 4, but not 2 or 3, significantly attenuated the MG132-induced increase in both mRNA and protein levels (*Figure 4A* and *B*). SP600125, an inhibitor of JNK phosphorylation, prevented the JNK phosphorylation by MG132 at both 5 and 10 μmol/L (*Figure 4C*). Z-ATAD, a caspase-12 inhibitor, attenuated the activation of caspase-12 by MG132 at 10, but not 2, μmol/L (*Figure 4D* and E). Cell viability analysed by 3-(4,5-dimethylthiazol-2-yl)-2,5-diphenol tetrazolium bromide (MTT) assay showed that siRNA targeting CHOP, but not SP600125 (5 μmol/L) or Z-ATAD (10 μmol/L) compound, prevented cell death induced by proteasome inhibition in rat-cultured cardiomyocytes (*Figure 4F*). Furthermore, consistent with the data of MTT assay, flow cytometry analysis showed that siRNA targeting CHOP, but not SP600125 or Z-ATAD, attenuated the apoptosis of cardiomyocyte induced by proteasome inhibition (*Figure 4G* and *H*).

3.4 Overexpression of glucose-regulated protein 78 attenuated endoplasmic reticulum stress and cell death by proteasome inhibition in cultured cardiomyocytes

Location of GRP78 overexpressed by adenovirus in cultured cardiomyocyte was almost consistent with that of protein disulphide isomerase, an ER-resident oxidoreductase (*Figure 5A*). The increase in GRP78 expression was confirmed by western blot analysis with the specific antibody of KDEL. Interestingly, GRP78 overexpression specifically inhibited the induction of CHOP, but not activation of caspase-12 or JNK (*Figure 5B–F*). Moreover, GRP78 overexpression dose-dependently decreased CHOP induction and increased cardiomyocyte viability (*Figure 5G–J*). Furthermore, the flow cytometry analysis also showed that overexpression of GRP78 attenuated apoptosis induced by proteasome inhibition in rat-cultured cardiomyocytes (*Figure 5K* and *L*). The overexpression of GRP78 combined with CHOP knockdown did not show additional effects on cardiomyocytes viability compared with GRP78 overexpression or CHOP knockdown alone (*Figure 5M*).

4. Discussion

The present study demonstrated that proteasome inhibitors, such as MG132 and epoxomicin, activated the ER stress-induced transcriptional factor ATF6, but not XBP1, without commeasurable expression of ER chaperone upon proteasome inhibition. Furthermore, proteasome inhibition induced cardiac apoptosis via CHOP-, but not JNK- or

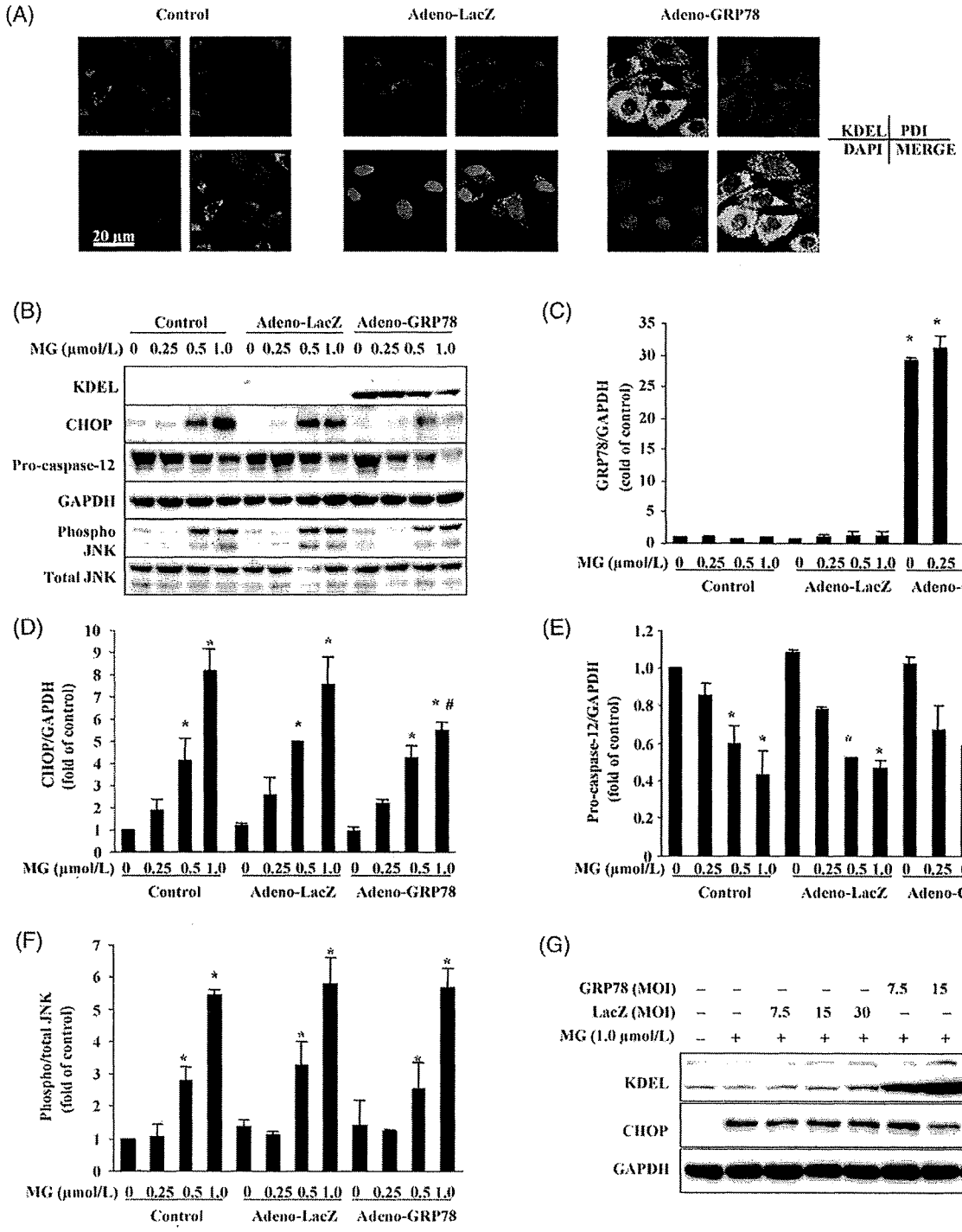

Figure 5 Overexpression of glucose-regulated protein (GRP) 78 reduced cardiomyocyte death by proteasome inhibition. (*A*) GRP78 was overexpressed by adenovirus at multiplicity of infection (MOI) 30 in cultured cardiomyocyte. Confocal fluorescence microscopy revealed that KDEL, PDI (protein disulphide isomerase) and DAPI were stained green, red and blue, respectively. (*B*) GRP78 expression, CCAAT enhancer-binding protein (C/EBP) homologous protein (CHOP) expression and activation of capase-12 were investigated after the treatment with MG132 (MG) (1.0 μmol/L) for 6 h at appropriate concentrations, while phospho-c-Jun-N-terminal kinase (JNK) was detected 1 h after MG administration. (*C–F*) Quantitative data of GRP78 expression (*C*), CHOP expression (*D*), casapase-12 activation (*E*) and JNK phosphorylation (*F*). (*G–I*) Representative (*G*) and quantitative (*H*, *I*) data for the expressions of endoplasmic reticulum chaperone (KDEL) and CHOP protein after GRP78 was overexpressed in a dose-dependent manner. MG (1.0 μmol/L) was administrated for 6 h. (*J–L*) Effects of overexpression of GRP78 on cardiomyocyte viability by 3-(4,5-dimethylthiazol-2-yl)-2,5-diphenol tetrazolium bromide (MTT) analysis (*J*) ($n = 6$ in each experiment) and cardiomyocytes apoptosis by flow cytometry (*K*, *L*) ($n = 3$ in each experiment) after MG (1.0 μmol/L) administration. (*M*) Effects of GRP78 overexpression combined with CHOP knockdown on cardiomyocyte viability by MTT analysis after proteasome inhibition ($n = 5$ in each group). Results of western blot and flow cytometry analysis represented three independent experiments, while the result of cell viability was from four independent experiments, respectively. (Asterisk) $P < 0.05$ vs. control; (Hash) $P < 0.05$ vs. MG (1.0 μmol/L).

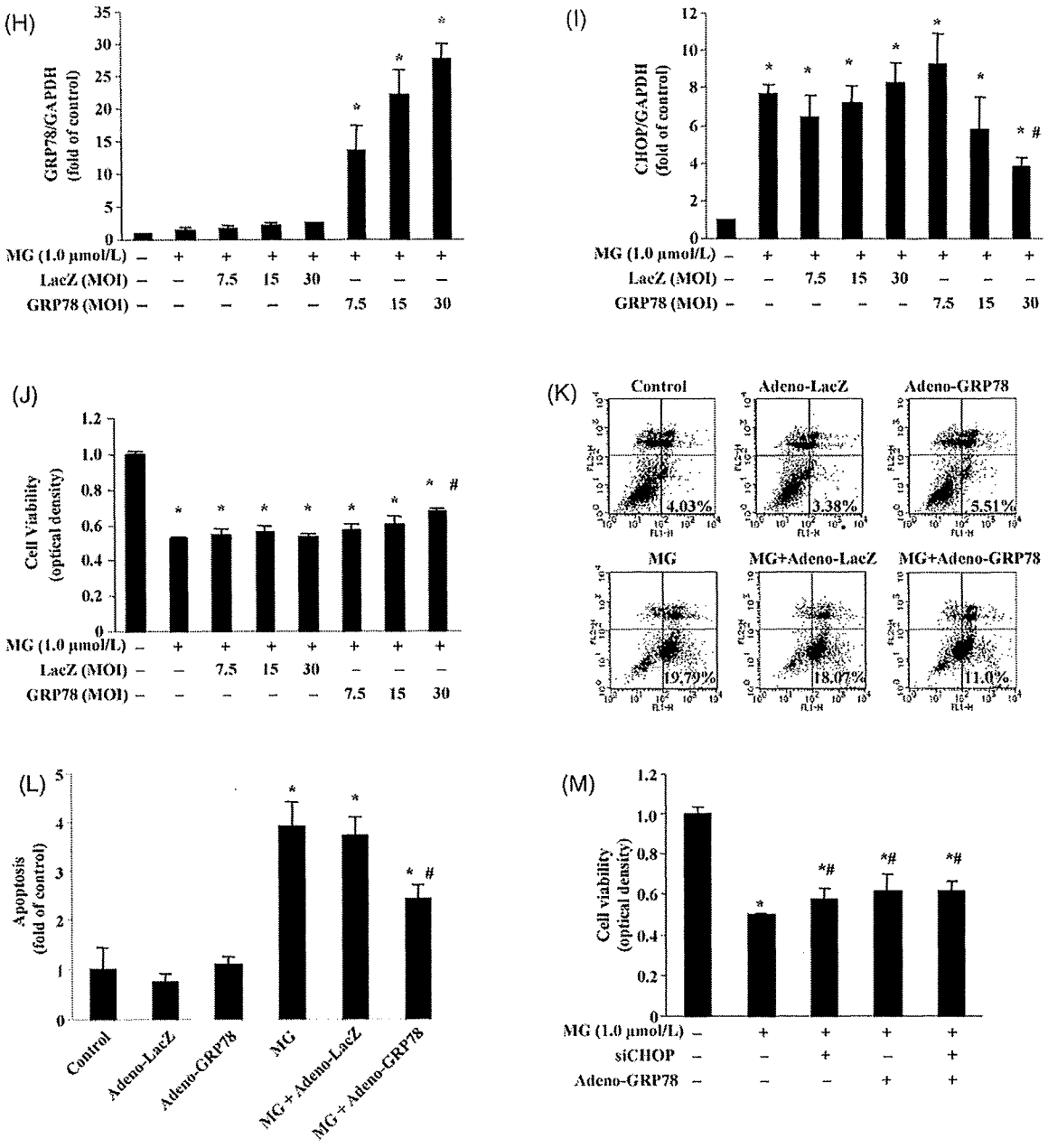

Figure 5 Continued.

caspase-12-, dependent pathway. Adenovirus-mediated GRP78 overexpression attenuated CHOP expression and rescued cardiomyocyte death by proteasome inhibition. These results suggest that proteasome inhibition caused ER stress without a compensatory increase in ER chaperones and induced cardiac apoptosis via the CHOP-dependent pathway. Supplement and/or pharmacological induction of GRP78 may be a potential therapeutic tool to attenuate cardiac damage by proteasome inhibition.

After proteasome inhibition, cleaved ATF6 protein in the nuclear fraction was increased, which might be due to the decrease in ATF6 degradation by proteasome inhibition and/or increase in the ATF6 cleavage.[18] However, consistent with the previous report,[19] we could not detect the increase of spliced XBP1 at either mRNA or protein level, suggesting that XBP1 was not activated by proteasome inhibition. Since overexpression of cleaved ATF6 could up-regulate ER chaperone expression,[20,21] ER chaperone should be induced due to the increase in cleaved ATF6 by proteasome inhibition. In our study, however, ER chaperons were not up-regulated after proteasome inhibition, suggesting there are some mechanisms that may prevent up-regulation of ER chaperone by cleaved ATF6. Since unspliced XBP1 protein acts as a dominant negative inhibitor of the spliced form and deactivates ATF6 by heterodimerization,[19,22-24] one possible mechanism is that increased protein levels of unspliced XBP1 probably due to the decelerated degradation by proteasome inhibition

may prevent the induction of ER chaperone. No compensatory increase in the ER chaperone may deteriorate the ER function to cope with ER stress when proteasome activity is inhibited (*Figure 6*).

In the present study, proteasome inhibition activated ER-initiated apoptotic signalling such as CHOP, caspase-12, and JNK. Using siRNA targeting CHOP and pharmacological inhibitors for caspase-12 and JNK, we found that CHOP knockdown partially, but significantly, inhibited cardiac apoptosis, while other pharmacological inhibitors did not. These findings suggest that CHOP, but not caspase-12 or JNK, mainly mediated cardiac apoptosis by proteasome inhibition. Recent research showed that the importance of three ER-initiated apoptotic signals is not equivalently involved in the pathophysiology in ER stress-related diseases.[25–27] Importantly, CHOP knockdown only partially prevented cardiomyocyte death by proteasome inhibition, suggesting that other mechanisms to induce cell death would be involved. Indeed, we have previously demonstrated that proteasome deactivation increased pro-apoptotic regulatory protein levels, such as p53 and Bax, and their knockdown also partially, but significantly, attenuated cardiac apoptosis.[15] These findings suggest that proteasome inhibition may cause cardiac apoptosis via the ER stress-dependent and -independent pathways.

We found overexpression of GRP78 could attenuate both CHOP expression and cell death by proteasome inhibition in cultured cardiomyocytes. In addition, the combination of GRP78 overexpression and CHOP knockdown did not show additional effects on preventing cardiomyocyte death, indicating that cell survival by GRP78 overexpression is predominantly through CHOP-dependent pathway. Further investigation is needed to elucidated why GRP78 specifically blocked CHOP induction among ER-initiated apoptotic signals. In the present study, although CHOP knockdown or GRP78 overexpression showed the small improvement of cell survival when cardiomyocytes were treated with proteasome inhibitors, these findings have some clinical relevance. Since patients will repeatedly receive the proteasome inhibitor for much longer time in the clinical settings, even a small size of improvement will exert the beneficial effects on the patients who need to receive the proteasome inhibitors.

We have previously demonstrated that both CHOP and GRP78 expression were induced in samples from human failing hearts and mouse failing hearts due to the pressure overload.[28] These findings suggest that ER stress may be involved in the pathogenesis in developing heart failure. Although we did not have the opportunity to check the ER-stress related signalling in the animal or human model when proteasome is inhibited, our *in vitro* data strongly suggest that proteasome inhibition may play an important role in the cardiomyocyte death via the ER stress-dependent pathways. The difference in the activation of ER stress-related signalling may be dependent on the pathophysiology of heart failure, and it is necessary to clarify how ER stress is involved in pathogenesis of cardiac diseases.

The ubiquitin-proteasome system is impaired in pathological cardiovascular conditions, such as ischaemia/reperfusion and failing hearts resulting from pressure overload.[15,29] Here, we found that proteasome inhibition induced ER-initiated apoptosis in cultured cardiomyocytes, supporting the idea that the impairment of the ubiquitin-proteasome system may play a crucial role in the development of heart disease. Bortezomib (PS-341) is clinically used as a novel class of anticancer agents against haematological malignancy and solid

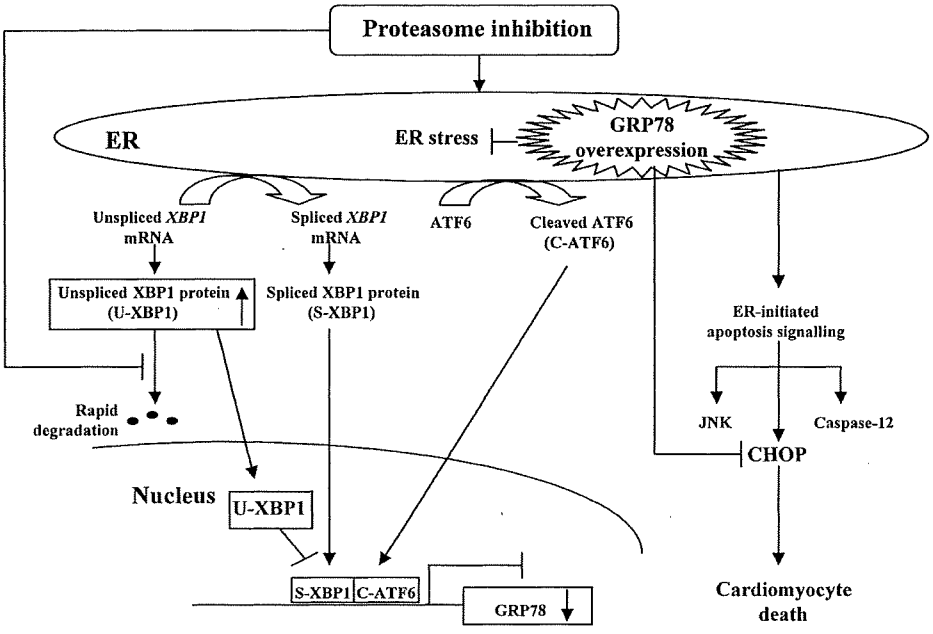

Figure 6 Schematic diagram of endoplasmic reticulum (ER)-chaperone glucose-regulated protein (GRP) 78 attenuating cardiomyocyte death by proteasome inhibition. Proteasome inhibition induces ER stress with the activation of activating transcription factor 6 (ATF6), but not X-box binding protein 1 (XBP1), in cardiomyocytes. Furthermore, proteasome inhibition activates ER-initiated apoptosis signalling such as CCAAT enhancer-binding protein (C/EBP) homologous protein (CHOP), JNK (c-Jun-N-terminal kinase) and caspase-12. Importantly, the expression of GRP78 was not enhanced probably due to the increased protein level of unspliced XBP1, which may further deteriorate ER stress. Overexpression of GRP78 attenuated cardiomyocyte death by proteasome inhibition via CHOP-dependent pathway. U-XBP1, S-XBP1, and C-ATF6 indicate unspliced XBP1, spliced XBP1, and cleaved ATF6, respectively.

tumour. Although bortezomib is not available currently in our hands, MG132 or epoxomicin used in the present study has similar characteristics as bortezomib to cause cell death via ER stress-related signalling.[30,31] Recently, some studies reported that the treatment with bortezomib was associated with cardiac dysfunction.[13,14] In addition, imatinib mesylate, a tyrosine kinase inhibitor used as an anticancer drug, was also reported to cause ER stress and heart failure.[32] Therefore, based on these findings, we need to monitor cardiac function carefully while using anticancer drugs that potentially disrupt protein quality control.

Conflict of interest: none declared.

Funding

This work was supported by a grant for Scientific Research from the Japanese Ministry of Education, Culture, Sports, Science and Technology (No. 17590731) and a grant from Japan Cardiovascular Research Foundation (No. 19390220).

References

1. Kaufman RJ. Stress signaling from the lumen of the endoplasmic reticulum: coordination of gene transcriptional and translational controls. *Genes Dev* 1999;**13**:1211–1233.
2. Shen J, Chen X, Hendershot L, Prywes R. ER stress regulation of ATF6 localization by dissociation of BiP/GRP78 binding and unmasking of Golgi localization signals. *Dev cell* 2002;**3**:99–111.
3. Calfon M, Zeng H, Urano F, Till JH, Hubbard SR, Harding HP *et al.* IRE1 couples endoplasmic reticulum load to secretory capacity by processing the XBP-1 mRNA. *Nature* 2002;**415**:92–96.
4. Yamamoto K, Yoshida H, Kokame K, Kaufman RJ, Mori K. Differential contributions of ATF6 and XBP1 to the activation of endoplasmic reticulum stress-responsive cis-acting elements ERSE, UPRE and ERSE-II. *J Biochem* 2004;**136**:343–350.
5. Hampton RY. ER-associated degradation in protein quality control and cellular regulation. *Curr Opin Cell Biol* 2002;**14**:476–482.
6. Oyadomari S, Mori M. Roles of CHOP/GADD153 in endoplasmic reticulum stress. *Cell Death Differ* 2004;**11**:381–389.
7. Morishima N, Nakanishi K, Takenouchi H, Shibata T, Yasuhiko Y. An endoplasmic reticulum stress-specific caspase cascade in apoptosis. Cytochrome c-independent activation of caspase-9 by caspase-12. *J Biol Chem* 2002;**277**:34287–34294.
8. Urano F, Wang X, Bertolotti A, Zhang Y, Chung P, Harding HP *et al.* Coupling of stress in the ER to activation of JNK protein kinases by transmembrane protein kinase IRE1. *Science* 2000;**287**:664–666.
9. Almond JB, Cohen GM. The proteasome: a novel target for cancer chemotherapy. *Leukemia* 2002;**16**:433–443.
10. Adams J. The development of proteasome inhibitors as anticancer drugs. *Cancer cell* 2004;**5**:417–421.
11. Kisselev AF, Goldberg AL. Proteasome inhibitors: from research tools to drug candidates. *Chem Biol* 2001;**8**:739–758.
12. Ludwig H, Khayat D, Giaccone G, Facon T. Proteasome inhibition and its clinical prospects in the treatment of hematologic and solid malignancies. *Cancer* 2005;**104**:1794–1807.
13. Voortman J, Giaccone G. Severe reversible cardiac failure after bortezomib treatment combined with chemotherapy in a non-small cell lung cancer patient: a case report. *BMC Cancer* 2006;**6**:129.
14. Enrico O, Gabriele B, Nadia C, Sara G, Daniele V, Giulia C *et al.* Unexpected cardiotoxicity in haematological bortezomib treated patients. *Br J Haemato* 2007;**138**:396–397.
15. Tsukamoto O, Minamino T, Okada K, Shintani Y, Takashima S, Kato H *et al.* Depression of proteasome activities during the progression of cardiac dysfunction in pressure-overloaded heart of mice. *Biochem Biophys Res Commun* 2006;**340**:1125–1133.
16. Minamino T, Gaussin V, DeMayo FJ, Schneider MD. Inducible gene targeting in postnatal myocardium by cardiac-specific expression of a hormone-activated Cre fusion protein. *Cir Res* 2001;**88**:587–592.
17. Shintani Y, Takashima S, Asano Y, Kato H, Liao Y, Yamazaki S *et al.* Glycosaminoglycan modification of neuropilin-1 modulates VEGFR2 signaling. *EMBO J* 2006;**25**:3045–3055.
18. Thuerauf DJ, Morrison LE, Hoover H, Glembotski CC. Coordination of ATF6-mediated transcription and ATF6 degradation by a domain that is shared with the viral transcription factor, VP16. *J Biol Chem* 2002;**277**:20734–20739.
19. Lee AH, Iwakoshi NN, Anderson KC, Glimcher LH. Proteasome inhibitors disrupt the unfolded protein response in myeloma cells. *Proc Natl Acad Sci USA* 2003;**100**:9946–9951.
20. Yoshida H, Matsui T, Yamamoto A, Okada T, Mori K. XBP1 mRNA is induced by ATF6 and spliced by IRE1 in response to ER stress to produce a highly active transcription factor. *Cell* 2001;**107**:881–891.
21. Li M, Baumeister P, Roy B, Phan T, Foti D, Luo S *et al.* ATF6 as a transcription activator of the endoplasmic reticulum stress element: thapsigargin stress-induced changes and synergistic interactions with NF-Y and YY1. *Mol Cell Biol* 2000;**20**:5096–5106.
22. Newman JR, Keating AE. Comprehensive identification of human bZIP interactions with coiled-coil arrays. *Science* 2003;**300**:2097–2101.
23. Yoshida H, Oku M, Suzuki M, Mori K. pXBP1(U) encoded in XBP1 pre-mRNA negatively regulates unfolded protein response activator pXBP1(S) in mammalian ER stress response. *J Cell Biol* 2006;**172**:565–575.
24. Yamamoto K, Sato T, Matsui T, Sato M, Okada T, Yoshida H *et al.* Transcriptional induction of mammalian ER quality control proteins is mediated by single or combined action of ATF6alpha and XBP1. *Dev Cell* 2007;**13**:365–376.
25. Kadowaki H, Nishitoh H, Ichijo H. Survival and apoptosis signals in ER stress: the role of protein kinases. *J Chem Neuroanat* 2004;**28**:93–100.
26. Nakagawa T, Zhu H, Morishima N, Li E, Xu J, Yankner BA *et al.* Caspase-12 mediates endoplasmic-reticulum-specific apoptosis and cytotoxicity by amyloid-beta. *Nature* 2000;**403**:98–103.
27. Tajiri S, Oyadomari S, Yano S, Morioka M, Gotoh T, Hamada JI *et al.* Ischemia-induced neuronal cell death is mediated by the endoplasmic reticulum stress pathway involving CHOP. *Cell Death Differ* 2004;**11**:403–415.
28. Okada K, Minamino T, Tsukamoto Y, Liao Y, Tsukamoto O, Takashima S *et al.* Prolonged endoplasmic reticulum stress in hypertrophic and failing heart after aortic constriction: possible contribution of endoplasmic reticulum stress to cardiac myocyte apoptosis. *Circulation* 2004;**110**:705–712.
29. Kostova Z, Wolf DH. For whom the bell tolls: protein quality control of the endoplasmic reticulum and the ubiquitin-proteasome connection. *EMBO J* 2003;**22**:2309–2317.
30. Davenport EL, Moore HE, Dunlop AS, Sharp SY, Workman P, Morgan GJ *et al.* Heat shock protein inhibition is associated with activation of the unfolded protein response pathway in myeloma plasma cells. *Blood* 2007;**110**:2641–2649.
31. Obeng EA, Carlson LM, Gutman DM, Harrington WJ Jr, Lee KP, Boise LH. Proteasome inhibitors induce a terminal unfolded protein response in multiple myeloma cells. *Blood* 2006;**107**:4907–4916.
32. Kerkela R, Grazette L, Yacobi R, Iliescu C, Patten R, Beahm C *et al.* Cardiotoxicity of the cancer therapeutic agent imatinib mesylate. *Nat Med* 2006;**12**:908–916.

Available online at www.sciencedirect.com
ScienceDirect
Biochemical and Biophysical Research Communications 368 (2008) 243–248
BBRC
www.elsevier.com/locate/ybbrc

Disappearance of the angiogenic potential of endothelial cells caused by Argonaute2 knockdown

Tomohiro Asai [a,*], Yuko Suzuki [a], Saori Matsushita [a], Sei Yonezawa [a], Junichi Yokota [a], Yasufumi Katanasaka [a], Tatsuhiro Ishida [b], Takehisa Dewa [c], Hiroshi Kiwada [b], Mamoru Nango [c], Naoto Oku [a]

[a] *Department of Medical Biochemistry and Global COE, University of Shizuoka School of Pharmaceutical Sciences, 52-1 Yada, Suruga-ku, Shizuoka 422-8526, Japan*
[b] *Department of Pharmacokinetics and Biopharmaceutics, Institute of Health Biosciences, The University of Tokushima, 1-78-1 Sho-machi, Tokushima 770-8505, Japan*
[c] *Materials Science and Engineering, Nagoya Institute of Technology, Gokiso-cho, Showa-ku, Nagoya 466-8555, Japan*

Received 5 January 2008
Available online 28 January 2008

Abstract

Argonaute2 (Ago2), a component protein of RNA-induced silencing complex, plays a central role in RNA interference. We focused on the involvement of Ago2 in angiogenesis. Human umbilical vein endothelial cells (HUVECs) stimulated with several growth factors such as vascular endothelial growth factor were used for angiogenesis assays. We applied polycation liposomes for transfection of small interfering RNA (siRNA) to determine the biological effects of siRNA for Ago2 (siAgo2) on HUVECs. The proliferation study indicated that siAgo2 significantly suppressed the growth of HUVECs compared with control siRNA. TUNEL staining showed a certain population of HUVECs treated with siAgo2 underwent apoptosis. Furthermore, the treatment with siAgo2 suppressed the tube formation of HUVECs and significantly reduced the length of the tubes. These present data demonstrate that siAgo2 inhibited indispensable events of angiogenesis *in vitro*. This is the first report suggesting that Ago2 is required for angiogenesis.

Keywords: Argonaute2; Angiogenesis; siRNA; Polycation liposomes

Double-stranded RNA (dsRNA) provokes sequence-specific gene silencing, commonly called RNA interference (RNAi) [1,2]. RNAi is a type of post-transcriptional gene silencing, and gene therapy using small interfering RNA (siRNA) is expected to be a novel treatment strategy [3]. For inducing RNAi, siRNA needs to be incorporated into an RNA-induced silencing complex (RISC). MicroRNAs (miRNAs), which are endogenous small non-coding RNAs that negatively regulate gene expression, are also incorporated into RISC for the cleavage or translational inhibition of the target mRNA [4]. Argonaute2 (Ago2) is a component protein of RISC and plays a central role in RNAi [5]. When a guide (antisense) strand of siRNAs or miRNA binds to its target mRNA, Ago2 expresses enzymatic activity to cleave the mRNA [6]. Ago2 is distinct from other Argonaute family members in the point that only Ago2-containing RISC is able to catalyze cleavage [5–7]. Ago2 is thus considered to be an indispensable protein for inducing RNAi. In addition, Ago2 cleaves the passenger strand of siRNAs, which facilitates the assembly of siRNAs into RISC [4,8]. On the other hand, Ago2-deficient mice show several developmental abnormalities such as a cardiac failure and a defect of neural tube closure [6]. Since these animals show an embryonic-lethal phenotype, Ago2 is essential for embryonic development.

Pathological angiogenesis is involved in diseases such as cancer [9]. Understanding of the mechanisms of angiogenesis

* Corresponding author. Fax: +81 54 264 5705.
E-mail address: asai@u-shizuoka-ken.ac.jp (T. Asai).

0006-291X/$ - see front matter © 2008 Elsevier Inc. All rights reserved.
doi:10.1016/j.bbrc.2008.01.074

leads to various antiangiogenic therapeutic modalities [10]. For instance, Avastin, a neutralizing antibody for vascular endothelial growth factor, is already used in clinical cancer chemotherapy [11]. While the participation of many proteins such as cytokines and signaling molecules in angiogenesis is well known, certain kinds of miRNAs have recently been shown to participate in angiogenesis [12]. Also, Dicer, a protein that cleaves long dsRNAs, is required for embryonic angiogenesis during mouse development [13]. Taken together, available information suggests that a miRNA system might be closely related to the regulation of angiogenesis. However, the involvement of Ago2 in angiogenesis is not known at all.

The present study is mainly focused on the possible involvement of Ago2, in addition to Dicer, in the regulation of angiogenesis. Our next concern is the application of Ago2 knockdown to antiangiogenic therapy. For establishment of RNAi therapy, a siRNA delivery system is quite important as well as a therapeutic target [14]. Polycation liposomes (PCLs), one of the non-viral types of vectors, possess the advantages of both cationic liposomes and polycations for gene delivery [15]. PCLs are simply prepared by modification of the liposomal surface with cetylated PEI (cetyl-PEI). Our previous study demonstrated that PCLs show various advantageous properties such as high transfection efficiency of plasmid DNA, low cytotoxicity, and applicability for *in vivo* use [15]. In this study, we optimized the formulation of PCLs for siRNA transfection and used such liposomes for analyzing the biological effects of Ago2 knockdown on angiogenesis.

Materials and methods

Preparation of siRNA/PCL complexes. Cetyl-PEI was synthesized as described previously [15]. Cholesterol was kindly provided by NFC Co. (Takasago, Hyogo, Japan). Dioleoylphosphatidylethanolamine (DOPE) was purchased from NOF Co. (Tokyo, Japan).

Cetyl-PEI, DOPE, and cholesterol (0.05:1:0.5 or 0 as a molar ratio) were dissolved in *tert*-butyl alcohol and freeze–dried. PCLs were produced by hydration of the lipid mixture with DEPC-treated RNase-free water. PCLs were sized by extruding them 10 times through a polycarbonate membrane filter having 100-nm pores. PCLs and siRNA solution were diluted with serum-free medium corresponding to the respective cell lines used. Then, PCLs and siRNA were mixed gently and incubated for 15 min at room temperature to form siRNA/PCLs complexes. The ratio of the nitrogen moiety of PCLs to the phosphate one of siRNA (*N/P* ratio) was varied from 18 to 30 for formulation screening. The particle size and ζ-potential of siRNA/PCLs complexes diluted with DEPC-treated water were measured by using a Zetasizer Nano ZS (Malvern, Worcs, UK). All siRNAs used in this study were purchased from Hokkaido System Science Co. (Hokkaido, Japan).

Cell cultures. HT1080 human fibrosarcoma cells (HT1080 cells) were cultured in DME/Ham F12 medium containing 10% fetal bovine serum (FBS; Sigma–Aldrich, St. Louis, MO), 100 U/ml penicillin (MP Biomedicals, Irvine, CA), and 100 μg/ml streptomycin (MP Biomedicals). HT1080 cells constitutively expressing EGFP (EGFP/HT1080 cells) had been previously established [16] and were cultured in the above medium supplemented with 100 μg/ml geneticin (Sigma–Aldrich). Human umbilical vein endothelial cells (HUVECs, Cambrex Bio Science Walkersville, Walkersville, MD) were cultured on gelatin-coated dishes containing endothelial growth medium-2 (EGM-2; Cambrex Bio Science Walkersville).

PCL-mediated transfection with siRNA. Cells were seeded and precultured overnight. The medium was then changed to fresh medium containing FBS but no antibiotics. Prepared siRNA/PCLs complexes (*N/P* ratio: 24 equiv) were added to the medium at a final concentration of 40 nM (as siRNA). After 4-h incubation, the siRNA/PCLs complexes were removed. These cells were subsequently incubated at 37 °C for additional periods of time as described for each experimental procedure.

Determination of the amount of siRNA taken into cells. The amounts of siRNA taken into cells were determined fluorometrically by using siRNA for Argonaute2 (siAgo2) labeled with 6-fluorescein-6-carboxamido hexanoate (FAM) at the 3′-terminal of its antisense strand. The nucleotide sequences of siAgo2 with a 2-nucleotide overhang (underline) were 5′-GC ACGGAAGUCCAUCUGAAUU-3′ (sense) and 5′-UUCAGAUGGAC UUCCGUGCUU-3′ (antisense). These sequences of siAgo2 correspond to the nucleotide region 1425–1443 and have been validated by G. Meister et al. [7].

HT1080 cells (3×10^4 cells/well) or HUVECs (5×10^4 cells/well) were seeded onto 24-well plates. After the cells had been cultured overnight, FAM-labeled siAgo2 (final concentration: 40 nM) in complex with PCLs was added to the cultures, which were then incubated for 4 h. The transfected cells were lysed with 2% reduced Triton X-100 containing protease inhibitors (2 mM PMSF, 200 μM leupeptin, 50 μg/mL aprotinin, and 100 μM pepstatin A). The fluorescent intensities of FAM were measured by using a spectrophotofluorometer (Wallac ARVO™ SX 1420 Multilabel Counter, Perkin-Elmer Life Sciences, Boston, MA) and corrected for protein amounts by using a BCA Protein Assay Reagent Kit (PIERCE Biotechnology, Rockford, IL) according to the manufacturer's instructions.

Evaluation of the RNAi efficiencies obtained with PCLs. The nucleotide sequences of the siRNA for EGFP (siEGFP) with a 2-nucleotide overhang (underline) were 5′-GGCUACGUCCAGGAGCGCACC-3′ (sense) and 5′-UGCGCUCCUGGACGUAGCCUU-3′ (antisense). The sequences of siEGFP correspond to the nucleotide region 118–141.

EGFP/HT1080 cells were seeded onto 24-well plates at the density of 6×10^4 cells/well and transfected with siEGFP complexed with PCLs. After these cells had been transfected, the cells were lysed at 48 h after culture. The fluorescence intensity of EGFP was measured with a spectrophotofluorometer and corrected for protein amounts. EGFP/HT-1080 cells were also transfected with siEGFP mixed with Lipofectamine™ 2000 (LFA2K, Invitrogen, Rockville, MD) according to the manufacturer's instructions. The transfection time schedule was similar to that used for the PCLs.

Cytotoxicity assay. EGFP/HT-1080 cells were seeded onto 96-well plates at the density of 1.2×10^4 cells/well and transfected with siEGFP. After 24-h incubation, Tetracolor ONE™ (Seikagaku, Tokyo, Japan) was added to each well in accordance with the manufacturer's instructions. The amount of formazan formed in 3 h was measured on a microplate reader (MTP-120, Corona Electric, Ibaraki, Japan) at a test wavelength of 492 nm and a reference wavelength of 630 nm.

RT-PCR. Total RNA was isolated by using an RNeasy Plus Mini Kit (Qiagen, Valencia, CA) at 8, 16 or 24 h post-transfection with siRNA. Complementary DNA was generated from total RNA samples (5 μg) by use of a Ready-To-Go T-primed First-Strand Kit (Amersham Biosciences, Piscataway, NJ). The PCR conditions were as follow: for Ago2, 94 °C for 5 min followed by 30 cycles of 94 °C for 30 s, 67 °C for 30 s, and 72 °C for 30 s and then 72 °C for 15 min; for β-actin and EGFP, 94 °C for 2 min followed by 20 cycles of 94 °C for 30 s, 55 °C for 30 s, and 72 °C for 1 min and then 72 °C for 10 min; and for GAPDH, 95 °C for 5 min followed by 20 cycles of 95 °C for 30 s, 60 °C for 30 s, and 72 °C for 1 min and then 72 °C for 10 min. The primers for Ago2 were 5′-TGAACAACATC CTGCTGCCCCAGGGC-3′ (sense) and 5′-TCATGTTCGATGCTGGC TGTCACGGAAGGG-3′ (antisense); for β-actin, 5′-TGACGGGGTCAC CCACACTGTGCCCATCTA-3′ (sense) and 5′-CTAGAAGCATTTGC GGTGGACGATGGAGGG-3′ (antisense), for EGFP, 5′-TACGGCAA GCTGACCCTGAAGTTC-3′ (sense) and 5′-CGTCCTTGAAGAAGAT GGTGCG-3′ (antisense); and for GAPDH, 5′-TGTTGCCATCAATGA CCCCTTC-3′ (sense) and 5′-AGCATCGCCCCACTTGATTTTG-3′ (antisense). The PCR products were applied onto 2.0% (β-actin, EGFP,